

CHARACTERIZATION AND MICROMECHANICAL INVESTIGATION OF RECYCLED
ASPHALT SHINGLE BINDER BLENDS

BY

ADAM C BEACH

THESIS

Submitted in partial fulfillment of the requirements
for the degree of Master of Science in Civil Engineering
in the Graduate College of the
University of Illinois at Urbana-Champaign, 2013

Urbana, Illinois

Adviser:

Professor William G. Buttlar

Abstract

The sustainability movement has established a firm foothold in the Civil Engineering profession. The use of recycled asphalt shingles (RAS) is the latest development in the world of asphalt pavement sustainability. The relative abundance of tear-off shingles and their high asphalt content is driving RAS usage in highway and airfield pavements. However, the ultimate objective of any pavement system is to provide a structural and functional roadway that can allow users to safely travel. Both state highway engineers and the general public need to be assured that the end product will not compromise performance. The performance grade of virgin asphalt binder will likely be altered when RAS is introduced into the asphalt mixture. The resulting Superpave material properties need to be predicted in order to assess that the mixture will perform adequately. In an experimental campaign which sought to investigate this, virgin PG 64-22 and PG 46-34 binders were blended with RAS binder at various percentages. Superpave material properties were measured and the performance grades determined for all binder blends. Prediction of complex shear modulus and flexural creep stiffness were then attempted using Hashin and Shtrikman's Arbitrary Phase Model. Use of calibration factors were found to accurately predict high temperature complex shear modulus, however, the model produced unexpected results for low temperature flexural creep stiffness. Micromechanical models that take into account the viscoelastic nature of asphalt would be expected to give an accurate prediction of material properties and should be pursued in further research. Finally, these micromechanical models should be incorporated into a practical system to aid designers in the maximization of recycled materials in asphalt pavements.

Dedicated to my grandfather, Professor C. Douglas Sutton

Acknowledgments

I would like to thank Professor William G. Buttlar, whose enthusiasm and support has enabled me to conduct this research. Additionally, my research group members have been instrumental in my success with this research topic, most specifically Brian Hill, who has been exceptionally helpful in lending his experience and guidance to me. I would also like to thank the research engineers at ATREL, especially Jim Meister, who spent numerous hours with me trying to perfect the RAS binder recovery process. Many thanks to Southwind RAS LLC, who not only provided the material for this project but has consistently kept me up to date on the latest RAS processing technologies. Lastly, I would like to thank the O'Hare Modernization Program for funding this research.

Table of Contents

Chapter 1: Introduction & Background.....	1
1.1 Asphalt Roofing Shingles	1
1.1.1 Composition	1
1.1.2 Organic Felts	2
1.1.3 Fiberglass Felts.....	2
1.2 Recycled Asphalt Shingles.....	3
1.2.1 Usage of Recycled Asphalt Shingles in Asphalt Pavement	3
1.2.2 Recycled Asphalt Shingles Advantages and Cost Benefit	4
1.2.3 Concerns with Including Recycled Asphalt Shingles in Asphalt Mixtures. ...	5
1.3 Problem Statement	6
1.4 Study Objectives	7
1.5 Scope of the Study.....	7
Chapter 2: Literature Review	8
2.1 Recycled Asphalt Shingle Binder Characterization	8
2.2 Micromechanical Models.....	11
2.2.1 Paul's Rule of Mixtures.....	12
2.2.2 Hashin and Shtrikman's Arbitrary Phase Geometry Model.....	13
Chapter 3: Recycled Asphalt Shingle Binder Characterization	15
3.1 Recycled Asphalt Shingle Source	15
3.2 Procedure for Extraction and Recovery	17
3.2.1 Extraction	17
3.2.2 Recovery using Rotovap	19
3.3 Binder Blending and Aging.....	20
3.4 High Temperature Testing	21
3.4.1 DSR Complex Shear Modulus Master Curves.....	21
3.4.2 High Temperature Performance Grade	24
3.5 Low Temperature Testing	25
3.5.1 BBR Creep Stiffness Master Curves	26
3.5.2 Low Temperature Performance Grading.....	28
Chapter 4: Investigation and Calibration of Micromechanical Models	30
4.1 Micromechanical Model Prediction of Complex Modulus Master Curves	31
4.1.1 Performance Graded 64-22 Base Binder.....	31
4.1.2 Performance Graded 46-34 Base Binder.....	34
4.2 Micromechanical Model Prediction of Creep Stiffness Master Curves.....	36
4.2.1 Performance Graded 64-22 Base Binder.....	37
4.2.2 Performance Graded 46-34 Base Binder.....	40
4.3 Use of Calibration Factors to Obtain Discrete Values	42
4.3.1 High Temperature Model Calibration	42
4.3.2 Low Temperature Model Calibration.....	45
Chapter 5: Summary.....	47
5.1 Conclusions	47
5.2 Recommendations	48
Chapter 6: References	49

Chapter 1: Introduction & Background

Recently, the general public has recognized the importance of building sustainable infrastructure. The push for sustainability in the construction industry can be met through the reduction of emissions, virgin material usage, and energy consumption. Recently, the pavement industry's approach to sustainability has involved the increased usage of recycled materials and the utilization of sustainable, new technologies (1). One of the most recent trends has been to recycle asphalt roofing shingles and to include them in asphalt mixtures.

1.1 Asphalt Roofing Shingles

For the last 85 years asphalt has been utilized as a critical component of manufactured roofing shingles. The cost of shingles has reduced significantly due to composition changes which include reductions in the overall weight of the shingle and efficiencies in the manufacturing process. In the 1980s, significant changes took place as the traditional three tab shingle was replaced with a single tab shingle. Fiberglass felt was introduced in the mid 1980s and the current designer shingles were introduced by the late 1980s. Today many different styles, patterns and colors of asphalt roofing shingles are manufactured worldwide. Despite rising material costs, the price of these shingles has remained stable due to efficiencies in the manufacturing process (2).

1.1.1 Composition

Asphalt roofing shingles consist of either organic or fiberglass felt that aids in maintaining the shape of the shingle and keeping the additional shingle components attached. This felt is impregnated with a weather-grade asphalt. This asphalt also contains mineral filler which provides stabilization for the asphalt and prevents it from becoming detached from the shingle felt. Sand granules are coated and pressed on the weatherface side of the shingles. Sand

granular provides color to the shingles and is primarily present for aesthetics. The reverse side of the shingle is coated with a backing dust to prevent them from sticking together during storage and transportation. Table 1 identifies approximate percentages of the components in manufactured asphalt roofing shingles (3).

Table 1: Typical Composition of Manufactured Asphalt Roofing Shingles

Component	Organic Shingles (% by weight)	Fiberglass Shingles (% by weight)
Asphalt Cement	30-36	19-22
Roofing Felt	2-15	2-15
Mineral Granules	20-38	20-38
Mineral Filler	8-40	8-40

1.1.2 Organic Felts

Organic felts are comprised of a virgin wood pulp and recycled cellulosic products. These shingles are able to maintain toughness, pliability and mechanical properties at low temperatures. Shingles manufactured with these felts will remain stiff even when exposed to higher roofing surface temperatures. They generally perform well under typical thermal cycles experienced in the United States or Canada. The primary disadvantage of organic shingles is that they are very susceptible to moisture (2).

1.1.3 Fiberglass Felts

Fiberglass felts are produced using a wet process that is similar to the production process of paper. Glass fibers are blended with a binder resin to form fiberglass mats. The mats have high tensile strength, good tear resistance and flexibility. The heavier fiberglass mats generally correlate in a tougher product. They also have good resistance to moisture and fire. However, they have the potential to be susceptible to cracking (2).

1.2 Recycled Asphalt Shingles

Incorporation of roofing asphalt shingles into hot mix asphalt has been proposed for over 30 years. Asphalt roofing shingles make up nearly two-thirds of the roofing market for both new homes and roof replacements. In 1998 it was estimated that over 11 million tons of shingle waste is generated annually. Waste generated from production of new roofing shingles accounts for 1 million tons of this waste (4). This waste was initially introduced into hot mix asphalt because it contains fewer contaminants. Thus, the recycling of asphalt shingles revolved around these “post-manufactured asphalt shingles” or manufactured asphalt shingle waste for about 20 years.

In recent years a strong push has been made for recycling and reuse of basic materials. Therefore, other options of recycling have been explored in depth. The ten million tons of shingles generated annually from demolished roofs have been considered a logical source for recycling. As opposed to post-manufactured shingles, "post-consumer asphalt shingles" or tear-off asphalt shingles have to go through additional sorting, inspection, testing and separation of undesirable materials. Asbestos testing is also required as it may be present in the roofing felt. Because the tear-off asphalt shingles come from a variety of sources, the variability of the material is generally higher than that of manufactured asphalt shingle waste. However, new processes and technologies have been developed so the end-product is a homogenous recycled asphalt shingle (RAS) mixture.

1.2.1 Usage of Recycled Asphalt Shingles in Asphalt Pavement

RAS mixtures have slowly been infiltrated into America's infrastructure. The primary goal of a RAS product is to replace a portion of virgin binder in the asphalt mixture. In the past, highway agencies have set specific weight limits on the percentage of manufactured asphalt

shingle waste allowed into a mixture. Recently, these restrictions have changed to an asphalt binder replacement (ABR) limit. These changes have reflected the agencies' concerns over potential problems that might be caused by the usage of RAS. In the advent of tear-off asphalt shingle production and the sustainability movement, state highway agencies have promoted research and testing that will allow for greater usage. Thus, the allowable ABR set by state highway agencies has risen in recent years. In addition to highways, airports have begun to incorporate RAS into mixtures at non-critical locations and there is an additional push for their inclusion in surface mixtures.

1.2.2 Recycled Asphalt Shingles Advantages and Cost Benefit

Primary general benefits of utilizing RAS in asphalt paving include:

- Reduced consumption of virgin materials
- Reduced emissions and energy consumption during processing and manufacturing of virgin materials
- Reduced by-product materials disposed in landfills
- Diminished consternation of public over-emissions
- Improved economic competitiveness of asphalt paving construction

The reduced consumption of virgin asphalt binder leads to significant cost savings for many parties involved (5). The following is based on information gathered from the city of Chicago and surrounding suburbs in April 2013. Landfills charge a fee of \$60/ton to deposit waste materials which include tear-off asphalt shingles. Local RAS producers, on the other hand, will charge a tipping fee of \$20/ton to deposit tear-off asphalt shingles. This results in a cost incentive for demolition teams to recycle the tear off asphalt shingles with the RAS producer. Southwind RAS LLC will sell "clean", processed RAS to contractors at a price of

\$45/ton, which results in a clear cost incentive for Southwind RAS LLC and other RAS producers. The price of asphalt binder is roughly \$560/ton as of February 2013. Assuming a 40% asphalt binder content in the shingle, recycled asphalt shingle binder from tear-off asphalt shingles would be valued at roughly \$115/ton, a \$445/ton price reduction when compared to virgin binder. This is a significant cost savings for the contractors and hiring agencies (6). Therefore, as long as the pavements continue to perform well, a clear economical incentive can be shown for all persons involved in the processing and consumption of RAS. The cost savings of RAS usage will continue to go up as higher limits for allowable ABR continues to increase.

1.2.3 Concerns with Including Recycled Asphalt Shingles in Asphalt Mixtures.

Manufactured asphalt shingle binder is significantly “stiffer” than traditional asphalt paving grades and behaves very differently. When shingles are placed on housing roofs for durations of 10 or more years this binder stiffness increases even more due to oxidative hardening of the asphalt concrete. Thus, including RAS in any asphalt mixture is likely to increase the viscosity of the binder phase and result in a stiffened asphalt mixture. This may lead to susceptibility to low temperature and fatigue cracking. Therefore, when RAS is utilized as a virgin binder replacement, it is necessary to choose an appropriate virgin binder grade that will offset the stiffness of the RAS binder. This technique is frequently called "grade bumping" and has been historically used when incorporating recycled asphalt pavement (RAP) as a binder replacement in asphalt mixtures.

Actual blending between RAS binder and virgin asphalt binder has not been researched in depth. The same thing can be said for the blending of RAP binder with virgin paving grades. However, this binder blending remains a critical issue for asphalt mixtures that contain recycled products. General consensus is that the mixing temperature of hot mix asphalt (HMA) needs to

be high enough so that the RAS binder will essentially "come off" the surface granular and fibers and fully blend with the virgin binder. Questions also arise as to the geometrical arrangement of asphalt binder within the mixture. This arrangement will impact the ductility of the materials which gives an indication of the asphalt mixtures resistance to cracking.

Variability can also be a concern when dealing with a recycled product that comes from a multitude of sources. Therefore, the end product may differ on a weekly basis depending on where the shingle source is located. In addition, RAS variability depends on the local climate, which will affect the service life of the asphalt shingle and how much oxidative hardening takes place. It is anticipated that warmer climates will have significantly stiffer RAS binders.

1.3 Problem Statement

The advent of the sustainability movement has provided a pathway for the rapid progression of RAS into American infrastructure. Specifically, RAS presents a clear economic and environmental benefit through its increased usage in pavement systems. However, the ultimate objective of any pavement system is to provide a structural and functional roadway that can allow users to travel safely. In order for this requirement to continually be met, the inclusion of RAS in pavements needs to be evaluated from a performance standpoint. Both state highway engineers and the general public need to be assured that the end product will not compromise performance. As mentioned previously, low temperature cracking can be a concern for pavements that contain RAS products. Virgin asphalt binder needs to be grade bumped to account for the stiff nature of RAS binder. The complex binder system that results needs to be able to resist both cracking and rutting by having the appropriate performance grade.

1.4 Study Objectives

The objectives of this thesis are to:

- Complete a thorough review of RAS binder characterization
- Investigate micro-mechanical models that may be able to predict the Superpave material properties of a RAS/virgin binder blend
- Characterize RAS binder and assess its influence on virgin asphalt binder
- Develop a method that can estimate key material properties of RAS/virgin binder blends used in the Superpave performance graded binder specification

1.5 Scope of the Study

A comprehensive literature review of RAS binder characterization was completed. The gathered information from this review aided in conducting preliminary RAS binder characterization of tear-off asphalt shingles obtained from Southwind RAS LLC, a supplier in Illinois. Binder blending with RAS binder was then completed for two different binder grades. These blends were aged using the Rolling Thin Film Oven (RTFO) and tested to obtain master curves for complex shear modulus and flexural creep stiffness as well as high and low temperature performance grades. Micromechanical models were then evaluated and utilized for estimation of Superpave material properties for a given binder blending percentage. A calibration scheme was investigated that could give a discrete estimate of Superpave material properties for a given RAS/virgin binder blend. Suggestions were also made for improvements to the model.

Chapter 2: Literature Review

2.1 Recycled Asphalt Shingle Binder Characterization

Several researchers have attempted to isolate RAS binder from other components (granular and mineral filler) in the asphalt shingle. Usually this is accomplished through an extraction and recovery procedure as outlined in AASHTO TP2. First, a solvent-binder mixture is isolated from other shingle components (aggregate, fiber or paper) using a centrifuge. A Rotovap device is then used in order to evaporate off the solvent which condenses on a cooling mechanism in a separate container. The result is recovered asphalt binder that is drained out of the evaporation flask. Texas A&M Transportation Institute (3) compiled a report that initially looked at the feasibility of obtaining the asphalt binder content of RAS, as well as recovering binder from RAS to determine the performance grade. Using the ignition oven method, tear-off asphalt shingles were shown to have a higher binder content (23 to 28 percent) than manufactured asphalt shingle waste (20 percent). This difference may be due to the loss of surface granulars during the service life of the roofing shingles. The variability in binder content was also shown to be lower for manufactured asphalt shingle waste. Extraction and recovery of the asphalt was very difficult due to the extremely stiff nature of the asphalt binder. The asphalt present on manufactured asphalt shingles is an air-blown AC 5 binder, which is much stiffer than a PG 76-22 binder, the stiffest binder used in Texas. The research team experienced difficulty when attempting to obtain the recovered tear-off asphalt shingle binder out of the beaker; the binder would not drain from the beaker, sometimes even at higher temperatures (greater than 200°C). The high temperature grade (PG 157 and PG 203 for two different sources) was determined using a specially purchased Dynamic Shear Rheometer (DSR), however it was not possible to determine the low temperature performance grade.

Bonaquist (7) studied various recycled binders and published a report with the Wisconsin Department of Transportation. He first verified the recommendation by NCHRP Report 9-12 to eliminate the need for Pressure Aged Vessel (PAV) aging of recycled binder. It was shown that RTFO aging of recovered RAS binder provided an excellent estimate of the AASHTO M20 grading of blended binders.

Because RAS binder is an air blown asphalt, it contains unique properties that will not allow conformance to Superpave grading requirements. For example, at high temperatures RAS binder is extremely stiff; thus, the high temperature performance grade is usually around 120°C to 150°C. On the low temperature side, the flexural creep stiffness value obtained from the Bending Beam Rheometer (BBR) crosses the 300 MPa flexural creep stiffness threshold at roughly -30°C while the m-value may not cross the 0.3 relaxation rate threshold until well above 0°C. Because of these complications at high and low temperatures, the researchers choose to use a binder blend of various virgin binder grades and linearly extrapolate to determine the critical Superpave material property temperatures for the RAS binder. Using binder blends up to 50% RAS binder, continuous performance grading was completed in accordance with AASHTO R29. It was found that northern RAS sources gave an extrapolated performance grade of PG 122.1-4.7 while southern RAS sources gave a slightly lower performance grade of PG 111.3-8.4. The error associated with these extrapolations however was deemed somewhat significant for most of the grading parameters. Therefore, this extrapolation may not be the best method for determining the performance grade of RAS binder.

Foxlow (8) at New Hampshire evaluated a RAS source that fractionates the shingles into sizes above the #50 sieve and below the #50 sieve, labeled +50 mesh and -50 mesh respectively. As mentioned with the previous study, the RAS binder had issues with traditional performance

grading using Superpave equipment. A separate asphalt mixture portion of the study compared mixtures containing RAS at an ABR of 10%. The performance grade changed from a PG 70-22 to a PG 76-22, showing a slight increase on the high temperature end.

Elseifi (5) did some similar binder blending with tear-off asphalt shingles using a new wet process. RAS is ground to ultrafine particles and is mixed with the virgin binder at high temperatures; this was successfully replicated in the lab. The performance grading results from this study is shown in Table 2. Two unmodified binders were blended between 10%-40% by weight of the binder. Increasing RAS percentages slightly increased the performance grade. The recommendations by the authors suggested up to 20% blending by weight of RAS.

Table 2. Performance Grade of RAS Blending by Elseifi (5)

Virgin Binder Grade	RAS Blending Amount	Resulting Performance Grade
PG 64-22	+10%	PG 70-16
PG 64-22	+20%	PG 70-16
PG 52-28	+10%	PG 52-22
PG 52-28	+20%	PG 58-28
PG 52-28	+40%	PG 58-22

NCAT(9) characterized manufactured asphalt shingle waste. They found a performance grade of PG 136-4. The authors blended a rejuvenator at various percentages to examine the effect on the RAS performance grade. They found that blending at 10% lowered the performance grade to PG 118-22 and blending at 20% lowered the performance grade to PG 94-28. Any addition of rejuvenator was shown to restore the material properties back to the desired PG 64-22.

Zhou(10) conducted a host of tests on both tear-off and manufactured asphalt shingle waste binder blending with both virgin asphalt binder and RAP binder. The authors investigated the effect of RAS binder on the performance grade of the RAS/virgin binder blend. At higher

RAS blending percentages it was often difficult to obtain the low temperature performance grade due to previously mentioned complications with the BBR. The average high temperature grade for the tear-off asphalt shingle binder was PG 175°C while the high temperature grade for manufactured asphalt shingle waste binder was found to be around PG 131°C. A significant finding with the binder blending was that the virgin/RAS binder blending was nonlinear, while previous studies along with the current one found the virgin/RAP binder blending to be linear. The authors also recommended that linear blending could be assumed up to 30% ABR.

2.2 Micromechanical Models

Past researchers have attempted to predict the rheological characteristics of asphalt mixtures using both empirical and theoretical models. Buttlar (11) utilized several micromechanical models in order to predict mixture stiffness at low temperatures using material properties obtained from both the aggregate and asphalt binder components.

Dave (12) also utilized these same micromechanical models for predicting the rheological properties of asphalt binders. Most notably, this work was done so a contractor could determine the presence of RAP in a mixture. The study involved blending virgin asphalt binder of varying grades with RAP binder and comparing how well the models predicted the complex shear modulus. The following models were considered:

- Paul's Rule of Mixtures (13)
- Hashin and Shtrikman's Arbitrary Phase Geometry Model (14; 15)
- Hashin's Composite Sphere Model (16)
- Christensen and Lo Generalized Self Consistent Scheme Model(17)
- Mori-Tanaka Model (18)
- Hirsch Model (19)

Some of these models predict upper and lower bounds for elastic material properties while others give a unique solution. The geometrical interpretation plays a significant impact on the construction of each model. For example, Buttlar (20) again used these same micromechanical models to better understand mastic behavior. It was found that the generalized self consistent scheme produced reasonable baseline reinforcement levels based on volume filling a soft asphalt matrix with rigid filler particles. The geometrical interpretation of this model allows an interaction between the matrix and equivalent homogenous material which is more realistic when modeling mastics. When considering binders, however, the geometrical phase and interface between materials is generally unknown. Therefore, only arbitrary geometrical phases which consider a range of physical interactions between the materials must be considered. For this reason, in order to accurately assess what the predicted Superpave material properties of a given asphalt binder blend will be, only two of the previously mentioned micromechanical models were considered: Paul's Law of Mixtures and Hashin and Shtrikman's Arbitrary Phase Geometry Model. Both provide arbitrary isotropic phase geometry with upper and lower bounds for the elastic material properties.

2.2.1 Paul's Rule of Mixtures

Paul's model defines upper and lower bounds for elastic material properties that were derived based on the principles of minimum potential and minimum complimentary energy. The two parameter model uses effective elastic moduli (shown in Equation 1 and Equation 2) for composite materials composed of irregular geometries.

$$\frac{1}{\frac{c_1}{K_1} + \frac{c_2}{K_2}} \leq K^* \leq K_1 c_1 + K_2 c_2 \quad \text{Equation 1}$$

$$\frac{1}{\frac{c_1}{G_1} + \frac{c_2}{G_2}} \leq G^* \leq G_1 c_1 + G_2 c_2 \quad \text{Equation 2}$$

Where:

K^*, G^* = Effective bulk and shear moduli of the composite, respectively

K_1, K_2 = Bulk moduli of phases 1 and 2, respectively

G_1, G_2 = Shear moduli of phases 1 and 2, respectively

c_1, c_2 = Volume fractions of phases 1 and 2, respectively

2.2.2 Hashin and Shtrikman's Arbitrary Phase Geometry Model

Hashin and Shtrikman derived improved bounds based on elasticity extremum principles. Derivations based on two-phase composites are shown for lower and upper bounds for bulk modulus in Equation 3 and Equation 4, respectively. The assumption is that the actual value will be between the two bounds (Equation 5).

$$K_L^* = K_1 + \frac{c_2}{\frac{1}{K_2 - K_1} + \frac{3c_1}{3K_1 + 4G_1}} \quad \text{Equation 3}$$

$$K_U^* = K_2 + \frac{c_1}{\frac{1}{(K_1 - K_2)} - K_2 + \frac{3c_2}{3K_2 + 4G_2}} \quad \text{Equation 4}$$

$$K_L^* \leq K^* \leq K_U^* \quad \text{Equation 5}$$

The bounds were also derived for complex shear modulus using commonly known substitutions of elastic material parameters (Equation 6 and Equation 7, with the actual value between the two bounds, shown in Equation 8).

$$G_L^* = G_1 + \frac{c_2}{\frac{1}{(G_2 - G_1)} + \frac{6(K_1 + 2G_1)c_1}{5G_1(3K_1 + 4G_1)}} \quad \text{Equation 6}$$

$$G_U^* = G_1 + \frac{c_1}{\frac{1}{(G_1 - G_2)} + \frac{6(K_2 + 2G_2)c_2}{5G_2(3K_2 + 4G_2)}} \quad \text{Equation 7}$$

$$G_L^* \leq G^* \leq G_U^* \quad \text{Equation 8}$$

Where:

K_L^* = Effective bulk modulus of the composite, lower bound

G_L^* = Effective shear modulus of the composite, lower bound

K_U^* = Effective bulk modulus of the composite, upper bound

G_U^* = Effective bulk modulus of the composite, upper bound

Dave (12) used Hashin and Shtrikman's Arbitrary Phase Model to predict the complex shear modulus of virgin asphalt binder blended with RAP. It was determined that the actual complex shear modulus of the blended material fell within the bounds given by the model. To make the model more practical, however, an empirical calibration factor S was used to predict a discrete value that was located within the upper and lower bounds. The equation to predict the complex shear modulus with the calibration factor is shown in Equation 9.

$$G^* = G_L^* + (G_U^* - G_L^*)S \quad \text{Equation 9}$$

Chapter 3: Recycled Asphalt Shingle Binder Characterization

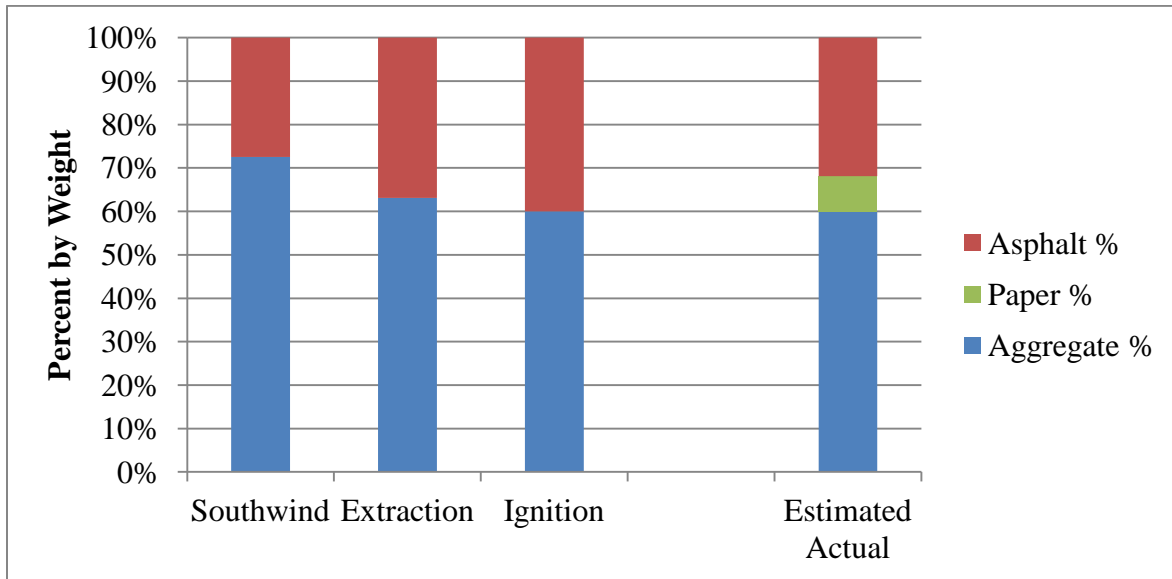
After reviewing the current literature, the first logical step for developing a method to characterize RAS binder blends was to first attempt to characterize the RAS itself and determine the performance grade for the RAS binder. As mentioned in the literature review, researchers in the past have had difficulty recovering RAS binder and determining its performance grade. Therefore, experimentation with available equipment and numerous trials were ran to determine the optimal method to accomplish this.

3.1 Recycled Asphalt Shingle Source

The RAS material utilized for this study was obtained from Southwind RAS LLC. Southwind RAS LLC is a company in the Chicago area that supplies RAS to clients such as the Chicago Department of Transportation, the Illinois Tollway and, recently, O'hare International Airport. With the approval for Illinois contractors to include tear-off asphalt shingles in mixtures in 2009, the use of RAS has increased tremendously. This is primarily due to the economic and environmental benefits previously mentioned. Therefore, Southwind RAS LLC has continued to expand to multiple locations and is the primary producer for RAS in Illinois. The material provided for this project was supplied by them from the Bartlett facility. Southwind RAS LLC utilizes custom designed grinders made specifically for processing tear-off asphalt shingles. The RG-1 Rotochopper produces a very consistent product. True gradations for the RAS product were obtained by Southwind RAS LLC. In addition, an extraction and ignition oven procedure was completed by the researchers to compare the gradations and asphalt contents. The asphalt content and gradations for the RAS product used are shown in Table 3 and Figure 1, Table 4 and Figure 2 respectively.

Table 3. Measured Component Percentages of RAS Material

	Southwind	Extraction	Ignition	Estimated Actual
Aggregate %	72.5%	63.1%	60.0%	60.0%
Asphalt %	27.5%	36.9%	40.0%	31.9%
Paper %	N/A	N/A	N/A	8.1%

**Figure 1. Measured Component Percentages of RAS Material****Table 4. True Gradation of RAS Material**

Sieve Size (English Units)	Sieve Size (SI Units)	Southwind	Extraction	Ignition
1/4	6.30	100.0	100.0	100.0
No. 4	4.75	95.0	92.7	97.5
No. 8	2.36	89.7	85.3	94.9
No. 16	1.18	71.6	73.3	80.6
No. 30	0.60	50.8	58.1	62.6
No. 50	0.30	43.9	52.3	56.7
No. 100	0.15	38.0	45.4	51.5
No. 200	0.08	30.0	36.5	42.9

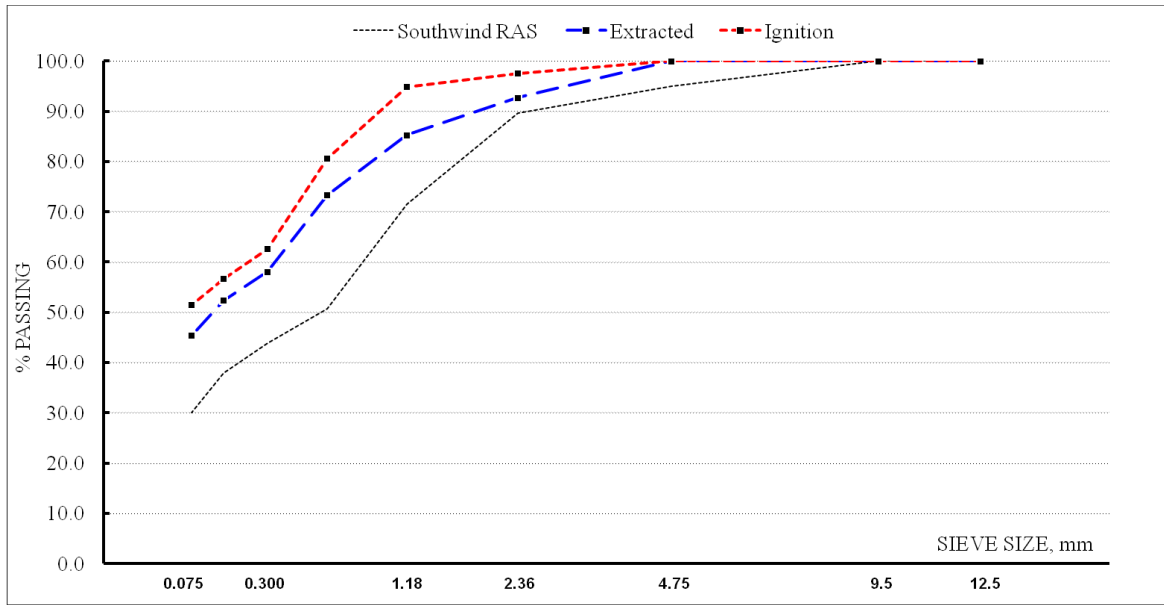


Figure 2. True Gradation of RAS Material

The gradations are fairly uniform and the material is generally regarded as fine, which was also discovered in the literature review. As expected, the asphalt binder percentage is significantly high. This greater percentage led to easier extraction of the binder from the other RAS material components.

3.2 Procedure for Extraction and Recovery

3.2.1 Extraction

A centrifuge was utilized in order to separate the RAS binder from the other components of the shingle. This centrifuge process was originally developed by Heritage Research Group and modified by researchers at Advanced Transportation Research and Engineering Laboratory and at the University of Illinois Urbana-Champaign. Southwind RAS LLC grinds the material to finer than 3/8" which generally allows for the binder to come off easier, and thus provides better binder blending. The dry material was fractioned to multiple sieve sizes. The number 4 sieve

contains the coarsest of the material and thus this material was utilized in the extraction recovery process to preemptively eliminate as many fines as possible.

Roughly 500 grams of course RAS material was placed on a set of sieves above the centrifuge. Entron solvent was poured over the RAS which traveled through a #16, #50 and #200 sieves and then through the centrifuge device. Configuration of the sieves with the centrifuge is shown in Figure 3. Five washes were typically done in this manner.



Figure 3. Configuration of Centrifuge Device

If the process were perfect, then only a solvent and binder combination would come out of the spout shown on the right side of the centrifuge, however, sometimes not all of the very

small fines get removed. Thus, the solvent binder solution is run through a 20 micron filter before going into the Rotovap device to further verify that all fine material had been removed.

3.2.2 Recovery using Rotovap

A Buchi Rotavapor R-210/R-215 was used for recovery of the RAS binder, shown in Figure 4. This device is also used in accordance with ASTM D504. After the solution was filtered, the solvent was evaporated off using a combination of heat and vacuum pressure. The solvent condenses on a cooled pipe and drips into a solvent flask on the other end of the device. The remaining material in the Rotovap flask is assumed to be solely RAS binder. The binder is drained from the flask in the oven for roughly 20-30 minutes at 200°C. Other researchers had difficulty draining the RAS binder from the flask; this was not noticed in this research study. Roughly 80-120 grams of RAS binder could be recovered in one extraction and recovery process compared to 30-40 grams obtained using methods from a typical RAP recovery (12).



Figure 4. Rotovap used for Recovery of RAS Binder

3.3 Binder Blending and Aging

RAS binder was blended with two separate virgin binders: PG 64-22 and PG 46-34. The difference in these virgin binders was expected to give an idea of RAS interaction with standard binders and assess when grade bumping may be needed. PG 46-34 was blended with 20%, 40%, and 70% RAS binder. PG 64-22 was also blended at these percentages with the addition of 10% RAS binder. These percentages would give an adequate picture of the RAS/virgin binder relationship with the assumption of total binder blending. The binders were mechanically blended using a rotary device as shown in Figure 5.



Figure 5. Mechanical Blender used to Mix Binders

After blending, the binders were RTFO aged in accordance with ASTM D 2872. As mentioned previously, researchers in the past have examined the impact of PAV aging recycled binders. The result has been that they tend to have little effect on the resulting performance grade. Therefore, the blended binders were not aged in the PAV before any of the low temperature testing.

3.4 High Temperature Testing

The RAS binder blends were tested using a Bohlin Gemini 2 Dynamic Shear Rheometer that is forced oven air temperature controlled and can test at temperatures above 100°C. This was important because RAS binder tested by researchers in the past had difficulty using a traditional water cooled DSR.

3.4.1 DSR Complex Shear Modulus Master Curves

The DSR was used to perform angular frequency sweeps from 0 to 100 radians/second at varying temperatures (46°C, 64°C, 82°C) on the RTFO aged binder blends. The recorded data was compiled using a Matlab program. The data from the various temperatures was then shifted to the reference temperature, in this case designated at 64°C. Temperature dependencies follow the WLF (Williams-Landel-Ferry) equation to calculate the temperature shift factor (21), shown in Equation 10.

$$\log \frac{a_T(T)}{a_T(T_0)} = -\frac{c_1(T - T_0)}{c_2 + (T - T_0)} \quad \text{Equation 10}$$

Where T_0 = reference temperature

c_1 = constant

c_2 = temperature constant

The shifted data was then fit to a sigmoidal function where $\alpha, \beta, \gamma, \delta$ are coefficients, shown in Equation 11.

$$\log(G^*) = \delta + \frac{\alpha}{1 + e^{\beta + \gamma(\log \omega_r)}} \quad \text{Equation 11}$$

Model constants and coefficients for both the WLF equation and the sigmoidal fit were found using the Microsoft Excel Solver tool which uses an optimization technique to reduce the least square error between the measured data and the fitted data. RTFO aged PG 64-22 virgin

binder blended with RAS binder master curves are shown in Figure 6. In addition, the PG 46-34 virgin binder blended with RAS binder master curves are shown in Figure 7.

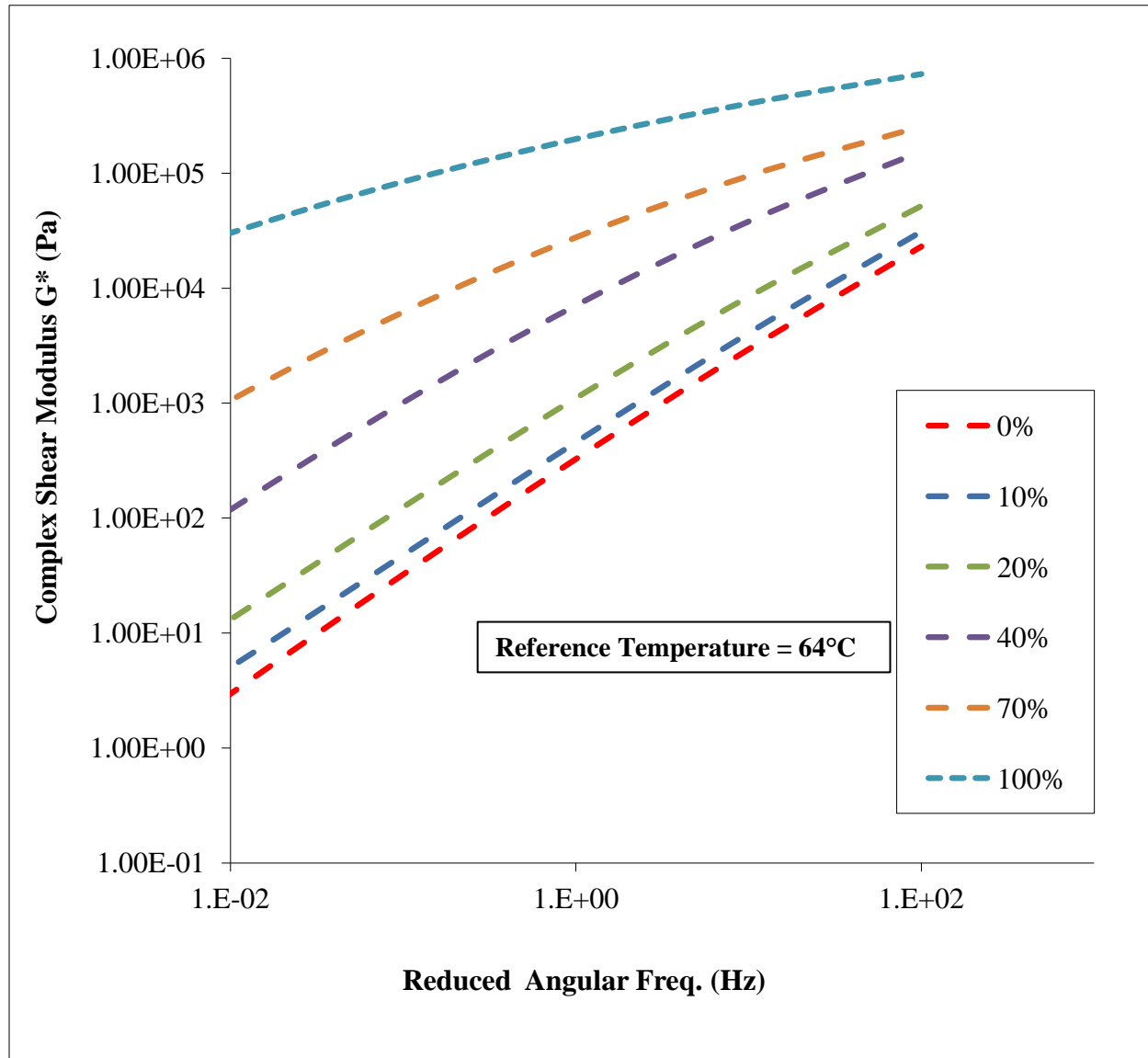


Figure 6. Complex Modulus Master Curves: PG 64-22 Blended with RAS Binder

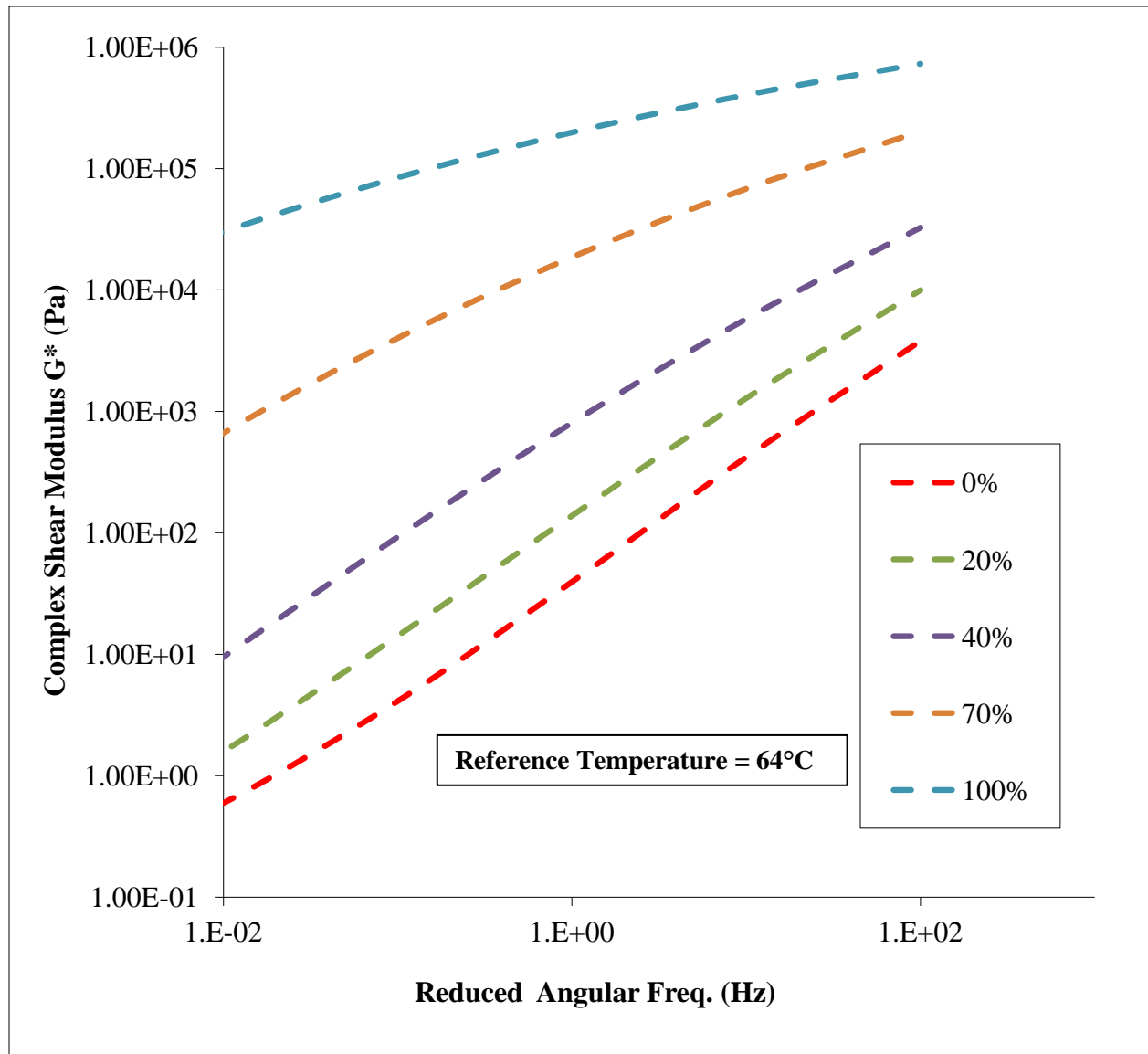


Figure 7. Complex Modulus Master Curves: PG 46-34 Blended with RAS Binder

A clear trend can be observed based on increasing RAS binder percentages. Complex shear modulus increases overall with increasing RAS binder. This can be attributed to the greater “stiffness” of the shingle binder. In addition, the slope of the master curves decreases with increasing RAS binder percentage, showing that RAS binder is less time-temperature sensitive than virgin asphalt binder. When comparing both virgin binders, it is evident that the PG

46-34 has a lower complex shear modulus than the PG 64-22 and thus shows lower complex shear modulus values when comparing similar blending percentages of RAS binder.

3.4.2 High Temperature Performance Grade

The high temperature performance grade for all RAS/virgin binder blends was also determined based on the RTFO aging condition. Superpave performance grading of binders requires that the binder conforms to the parameters shown in Table 5. The lowest temperature which passes both Superpave criteria is the high temperature performance grade.

Table 5. High Temperature Superpave Performance Grading Conformance

Aging Condition	Parameter	Value
Original Virgin Binder	$G^*/\sin(\delta)$	1 kPa
RTFO Aged Binder	$G^*/\sin(\delta)$	2.2 kPa

Past researchers have shown that the critical value for high temperature DSR testing is consistently in the RTFO aged condition. This was verified with several binder blends, therefore to save time, all other binder blends were graded based only on the RTFO aged condition. Figure 8 displays the effect of RAS binder blending percentage on the high temperature performance grade of the PG 64-22 and PG 46-34 base binders.

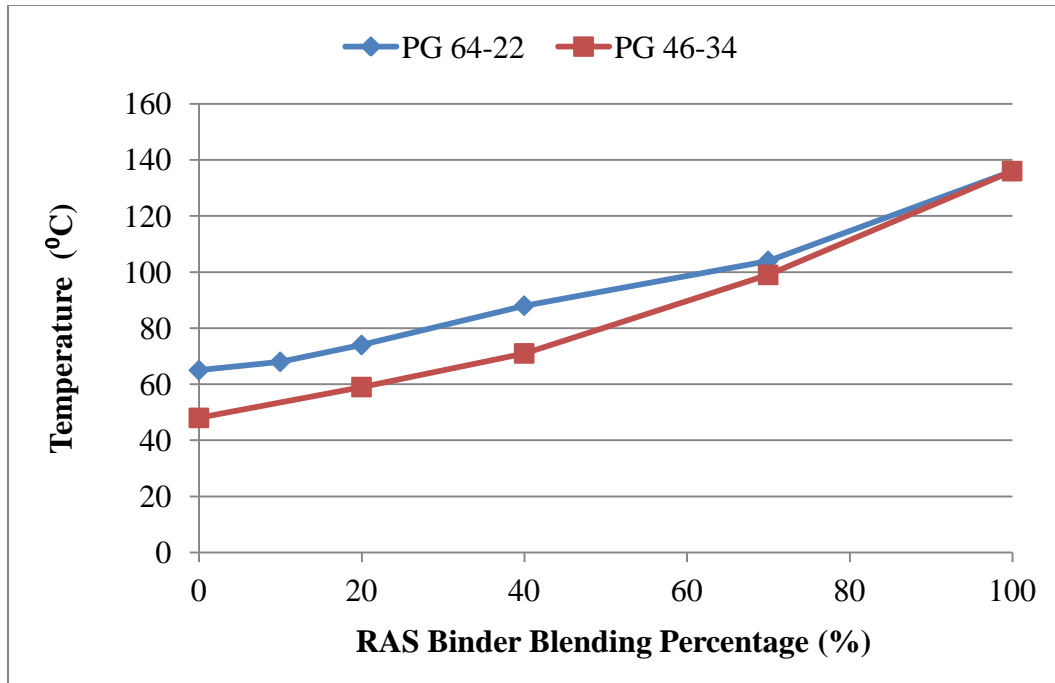


Figure 8. High Temperature Performance Grades: PG 64-22 and PG 46-34

The above figure shows the somewhat non-linear trend throughout the blending range, which is consistent with other researchers. Also consistent with other researchers is that linear blending occurs up to 40% RAS blending percentage. Greater non-linearity occurs with the PG 46-34 which was to be expected due to the softer nature of this binder.

3.5 Low Temperature Testing

The RAS binder blends were tested using a Bending Beam Rheometer (BBR) in accordance with ASTM D6648. As previous researchers have noted, it is difficult to test recovered RAS binder within specification using the BBR. In order to work around these issues, the 980kn creep load was adjusted at lower temperatures so the specimen would not break. In most cases the load was lowered to 500kn. Although this technique is not within the ASTM specification, reasonable creep stiffness values were still obtained using this technique.

3.5.1 BBR Creep Stiffness Master Curves

Figure 9 and Figure 10 show the creep stiffness master curves for virgin PG 64-22 and PG 46-34 blended with RAS binder respectively. The most prominent trend that can be observed from the creep stiffness master curves for both cases is the slope. RAS binder reduces the time-temperature susceptibility of the binder. This will result in a decreased m-value, which is an indication of the ability of the binder to relax induced thermal stresses. Therefore, RAS binder will have difficulty dissipating energy caused by thermal stress build up in the pavement. This will increase the low temperature performance grade of the RAS binder.

The creep stiffness master curves show little consistency in terms of creep stiffness values among blended RAS binder percentages. In general, it appears that the RAS binder has lower creep stiffness at lower loading times. This may be due to the elastic nature of the RAS binder, which deflects more when the initial load is applied. However, since the RAS has less time-temperature susceptibility, the creep stiffness master curve is significantly flatter when compared to virgin binders. Thus, at longer loading times the virgin binder will gradually flow, causing greater deflections over time which results in lower creep stiffness. The creep stiffness and m-value measurements are taken at 60 seconds to determine the performance grade of the binder. Therefore the observations noted should clearly be taken into account when observing the effect of RAS binder on virgin binder performance grades.

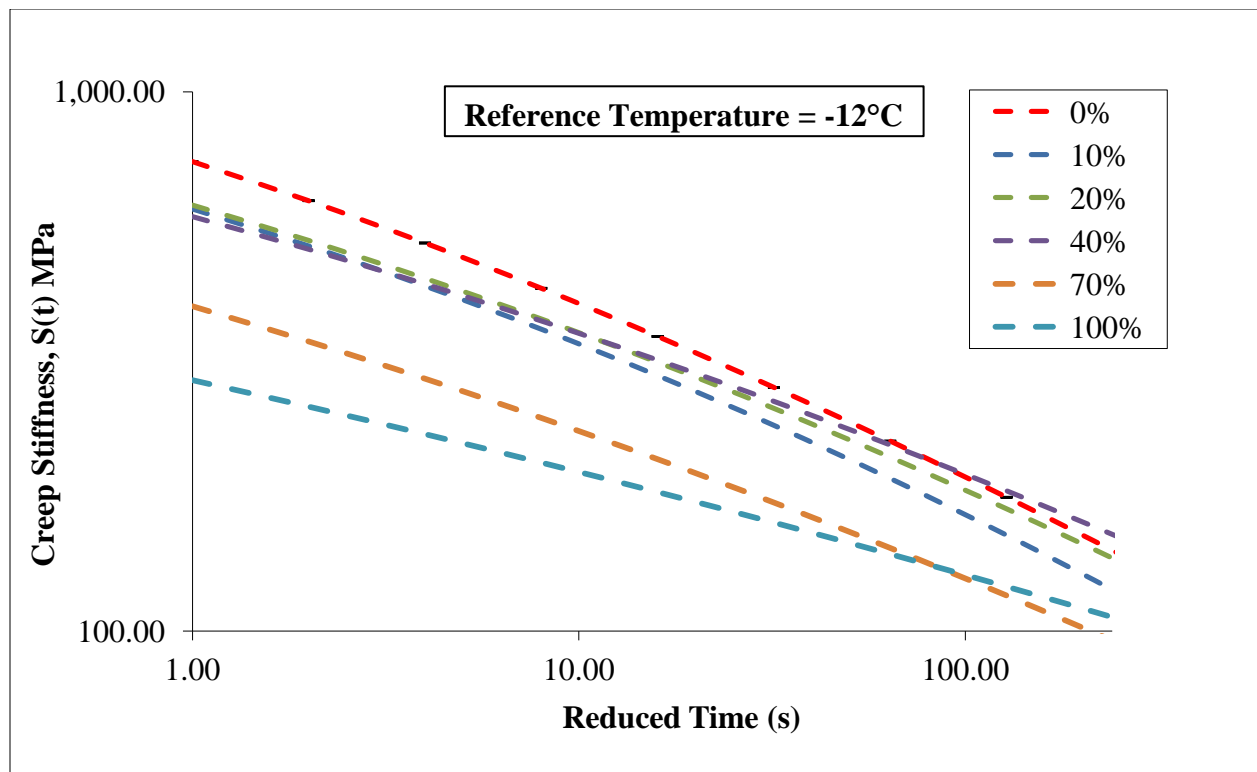


Figure 9. Creep Stiffness Master Curves: PG 64-22 Blended with RAS Binder

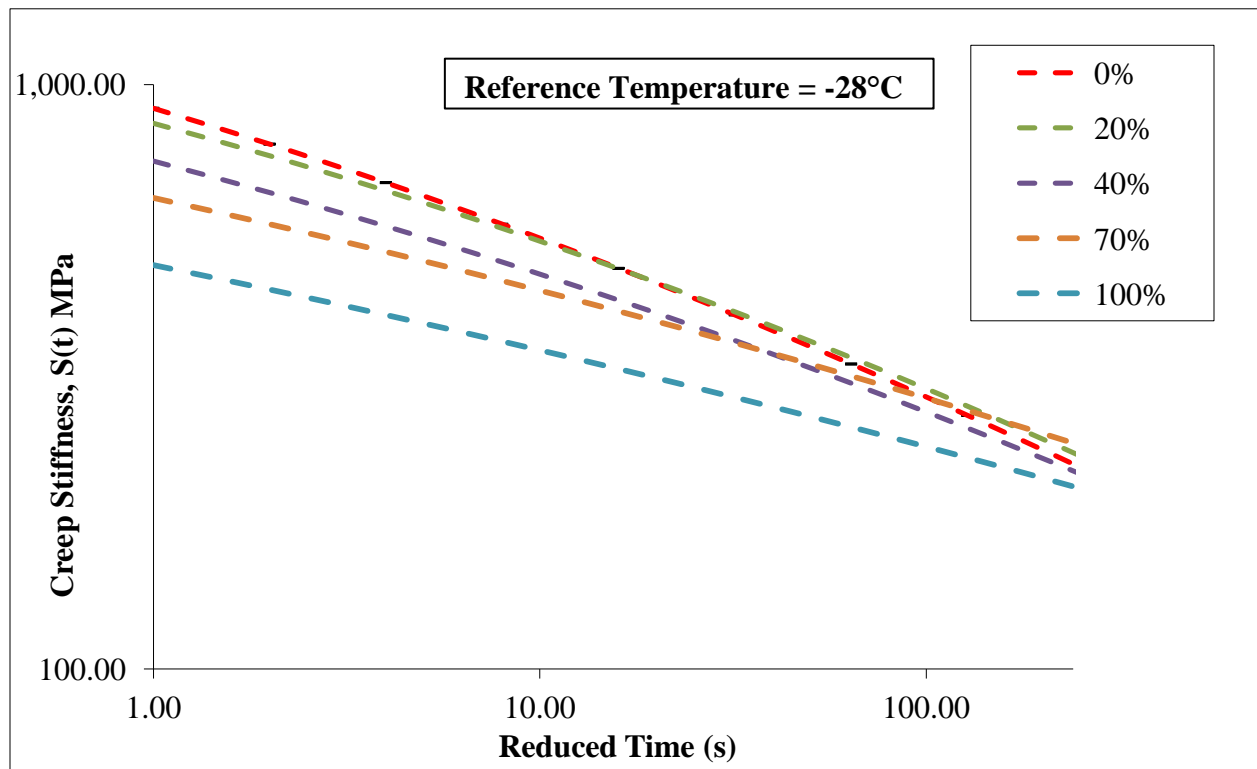


Figure 10. Creep Stiffness Master Curves: PG 46-34 Blended with RAS Binder

3.5.2 Low Temperature Performance Grading

The low temperature performance grade for all RAS/virgin binder blends was also determined based on the RTFO aging condition. Superpave performance grading of binders requires that binder conforms to the parameters shown in Table 6. The m-value is the tangential slope of the creep stiffness master curve. The highest temperature which passes both criteria is the low temperature performance grade.

Table 6. Low Temperature Superpave Performance Grading Conformance

Aging Condition	Parameter	Value
PAV Aged Binder	Stiffness @ 60 seconds	300 MPa
PAV Aged Binder	m-value @ 60 seconds	0.3

Past researchers have observed minimal differences between the RTFO aged and PAV aged conditions when one of the blended binders is a recycled binder. Therefore, BBR specimens were tested in the RTFO aged condition to save time. Figure 11 shows the effect of RAS binder blending percentage on the low temperature performance grade of PG 64-22 and PG 46-34. A non-linear trend throughout the blending range was observed, which is consistent with the high temperature performance grading. Also consistent with past researchers is that linear blending occurs up to 40% binder blending. Also, as expected, greater non-linearity again occurs with the PG 46-34.

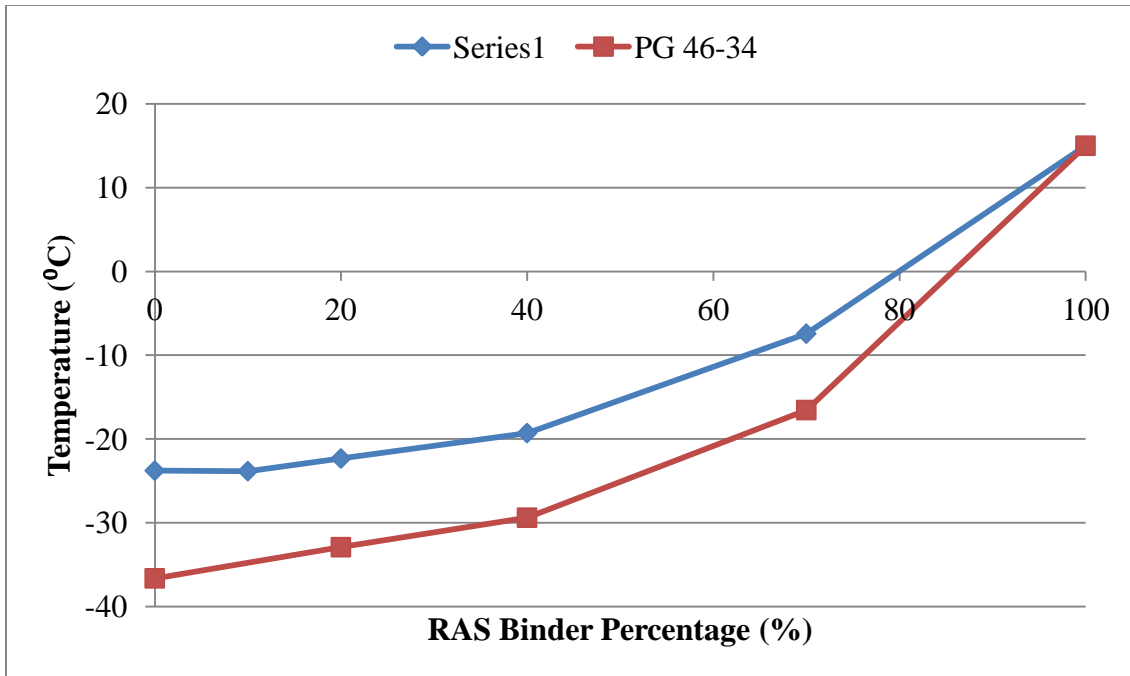


Figure 11. Low Temperature Performance Grades: PG 64-22 and PG 46-34

Chapter 4: Investigation and Calibration of Micromechanical Models

Micromechanical models which may help to predict material parameters of the multi-phase binders were investigated. The two models investigated initially were Paul's Rule of Mixtures and Hashin and Shtrikman's Arbitrary Phase Geometry Model. The master curve complex shear modulus data previously presented which was obtained from the DSR was used to evaluate these models. Figure 12 displays a slice in time (10 Hz) and temperature (64°C) which shows the bounds of both micromechanical models with the measured complex shear modulus. The bounds based on Hashin and Shtrikman's model indicate a slightly tighter control on the complex shear modulus. The measured data still stay within the bounds of this predictive model, indicating that Hashin and Shtrikman's model provides more precision but accurately portray the true phase geometry. Therefore, further analysis of model behavior was investigated using this Hashin and Shtrikman's Arbitrary Phase Model.

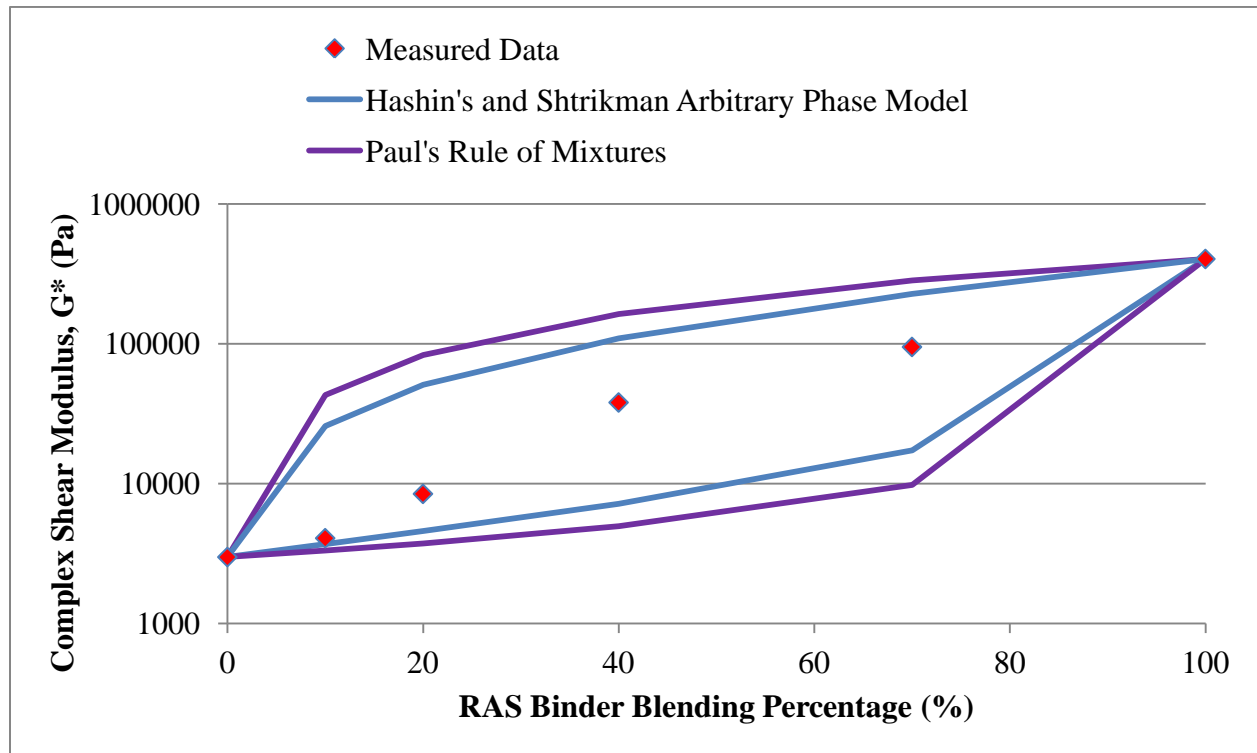


Figure 12. Complex Modulus for various RAS Blending Percentages at 64°C and 10 Hz

4.1 Micromechanical Model Prediction of Complex Modulus Master Curves

The complex shear modulus master curves were compared with Hashin and Shtrikman's Arbitrary Phase Model prediction. Complex shear modulus values were taken for both the virgin binder and RAS binder phases at varying frequencies and at the master curve reference temperature (64C) in order to develop the upper and lower bound curves. This method is a way to obtain reasonable predictions using the elastic material parameters that are established with this micromechanical model.

4.1.1 Performance Graded 64-22 Base Binder

Hashin and Shtrikman's model was first used to predict complex shear modulus values for PG 64-22 base binder blended with 10%, 20%, 40% and 70% RAS binder shown in Figure 13, Figure 14, Figure 15, and Figure 16 respectively. The measured data is consistently in between the upper and lower bound, showing the model provides a reasonably accurate prediction of the complex shear modulus. The other primary observation is that the measured complex shear modulus data tends to converge toward the upper bound with increasing binder blending percentage. This observation will be discussed in detail later, when calibration factors are taken into consideration.

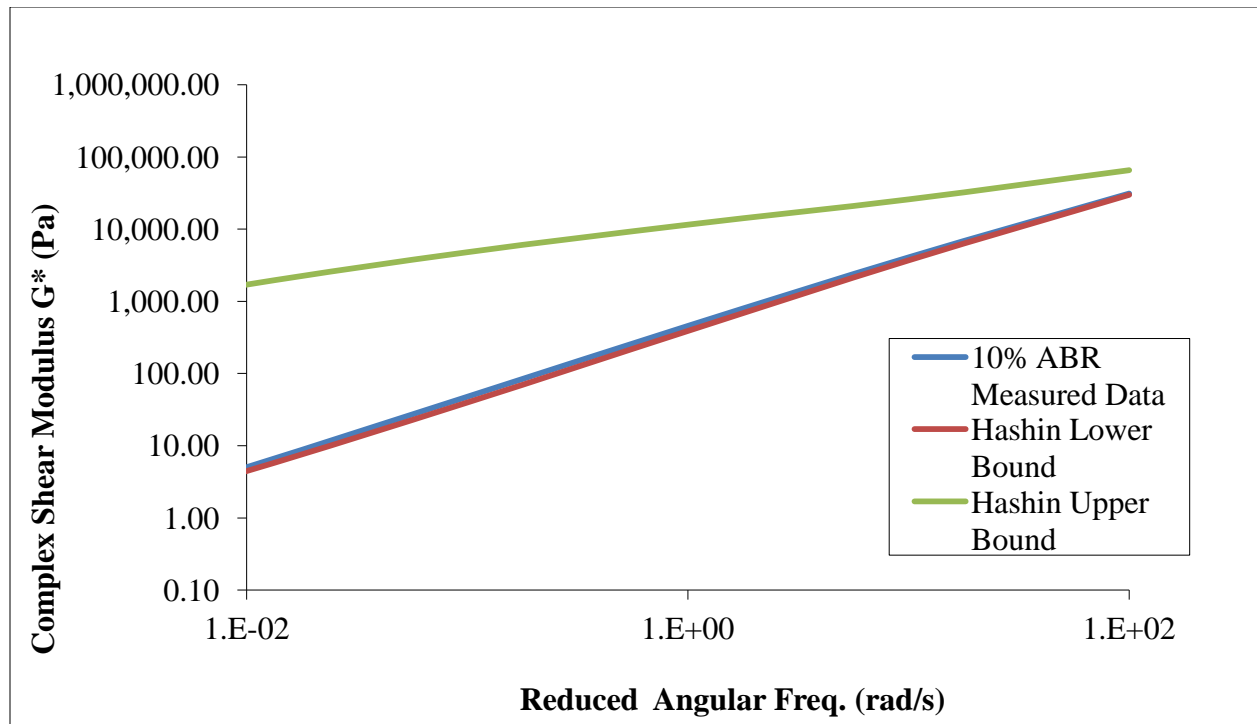


Figure 13. Complex Modulus Prediction of PG 64-22 with 10% RAS Binder Blending

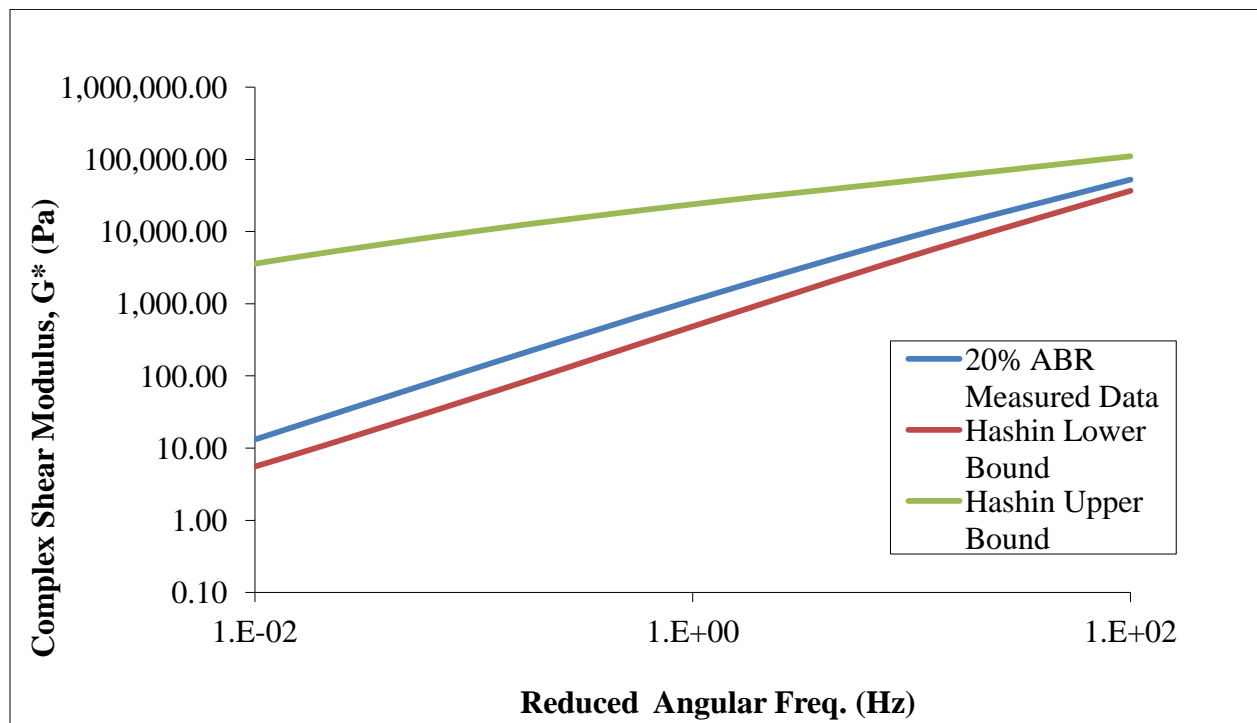


Figure 14. Complex Modulus Prediction of PG 64-22 with 20% RAS Binder Blending

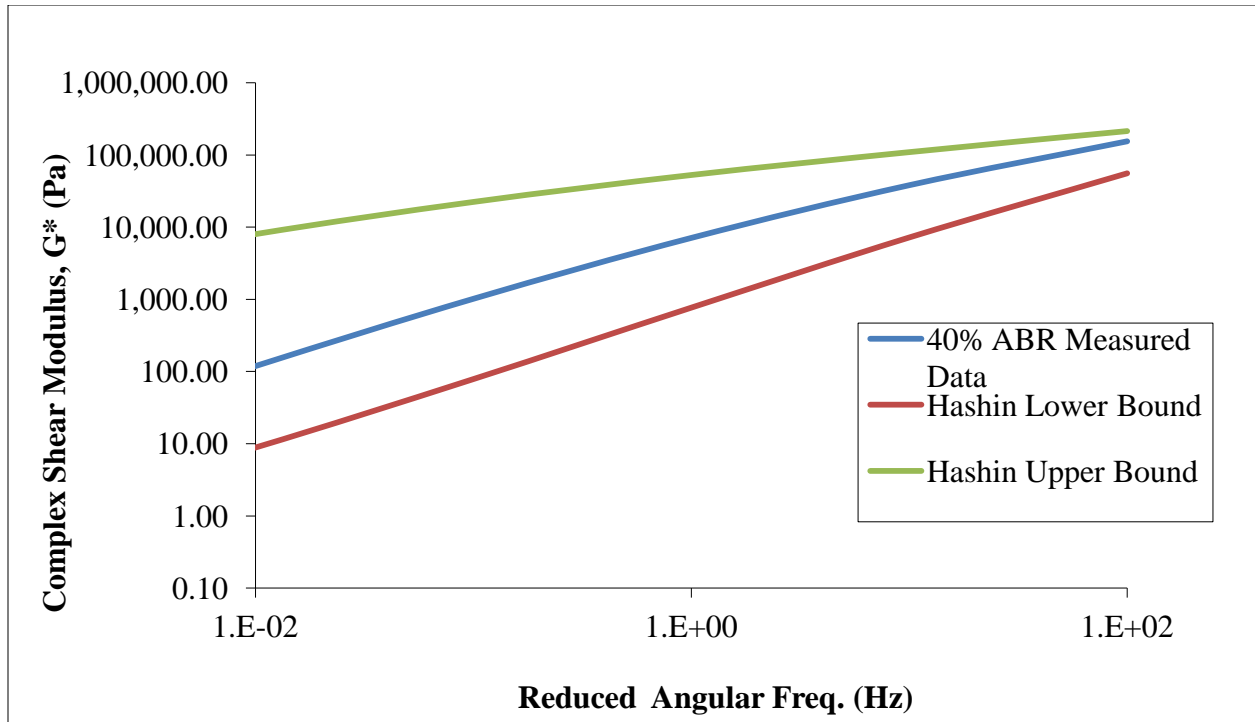


Figure 15. Complex Modulus Prediction of PG 64-22 with 40% RAS Binder Blending

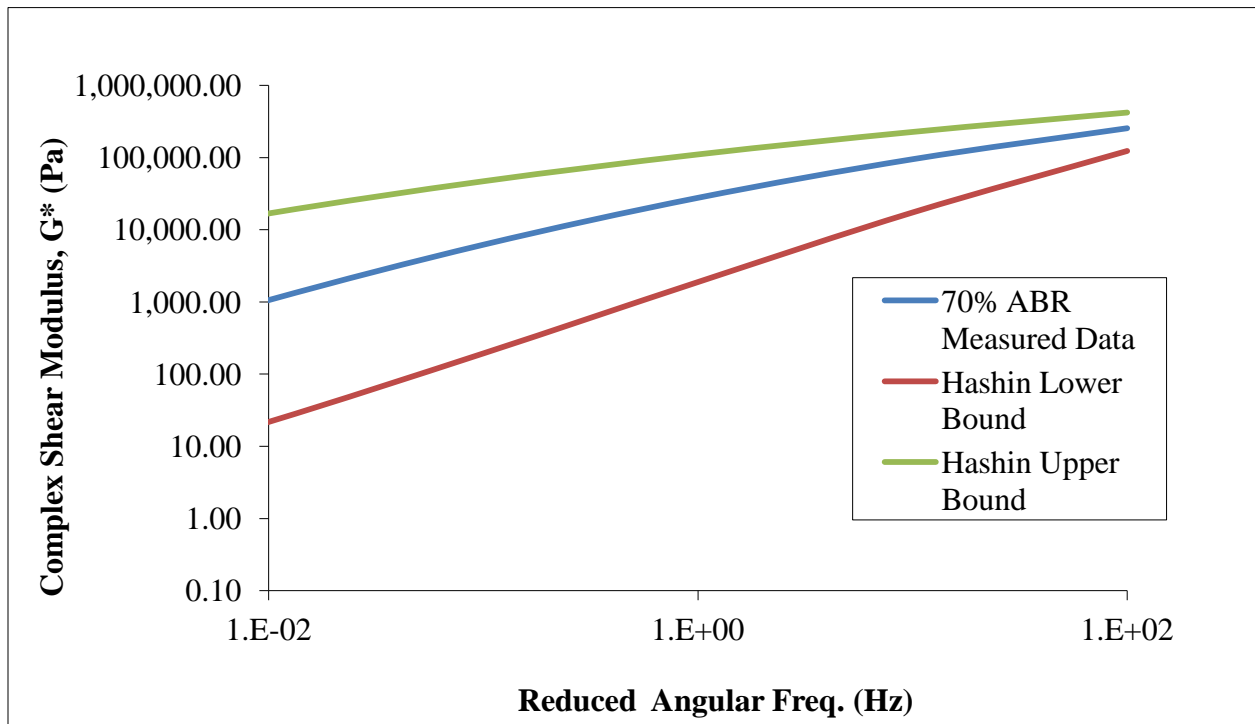


Figure 16. Complex Modulus Prediction of PG 64-22 with 70% RAS Binder Blending

4.1.2 Performance Graded 46-34 Base Binder

Similar trends noted above for PG 64-22 binder were also observed with PG 46-34 binder. Figure 17, Figure 18, and Figure 19 show PG 46-34 base binder blends with RAS binder at 20%, 40%, and 70% blending respectively.

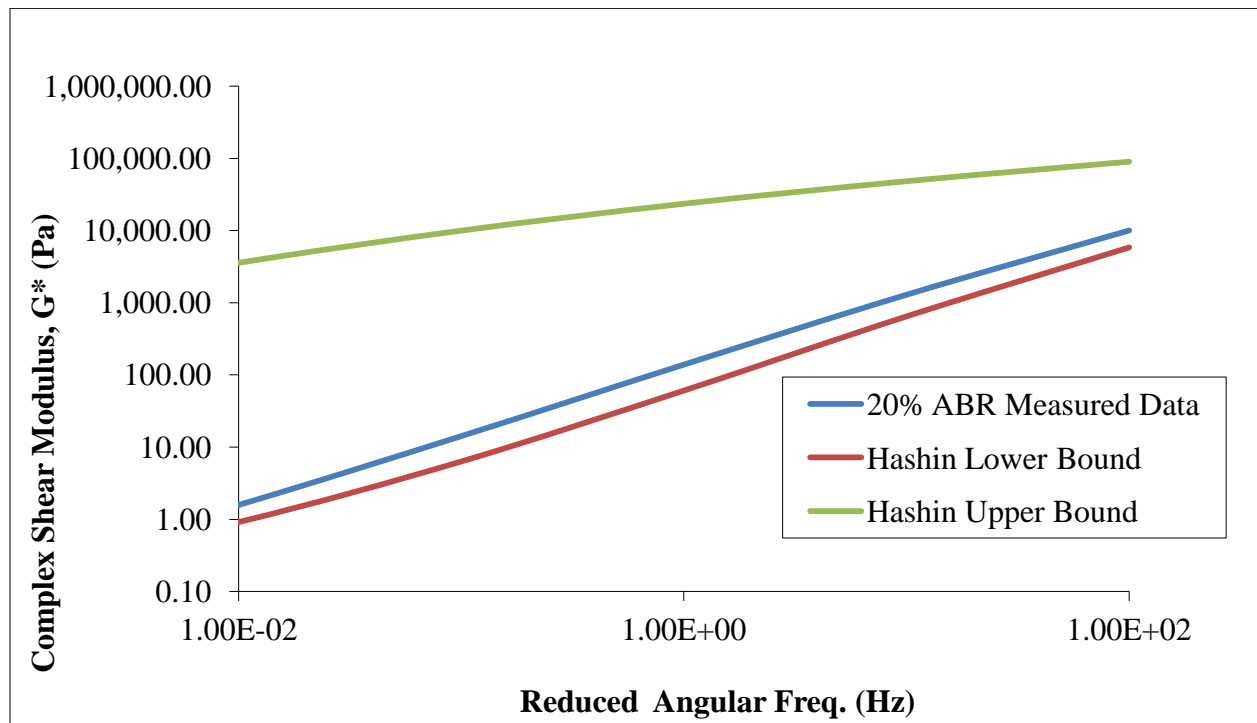


Figure 17. Complex Modulus Prediction of PG 46-34 with 20% RAS Binder Blending

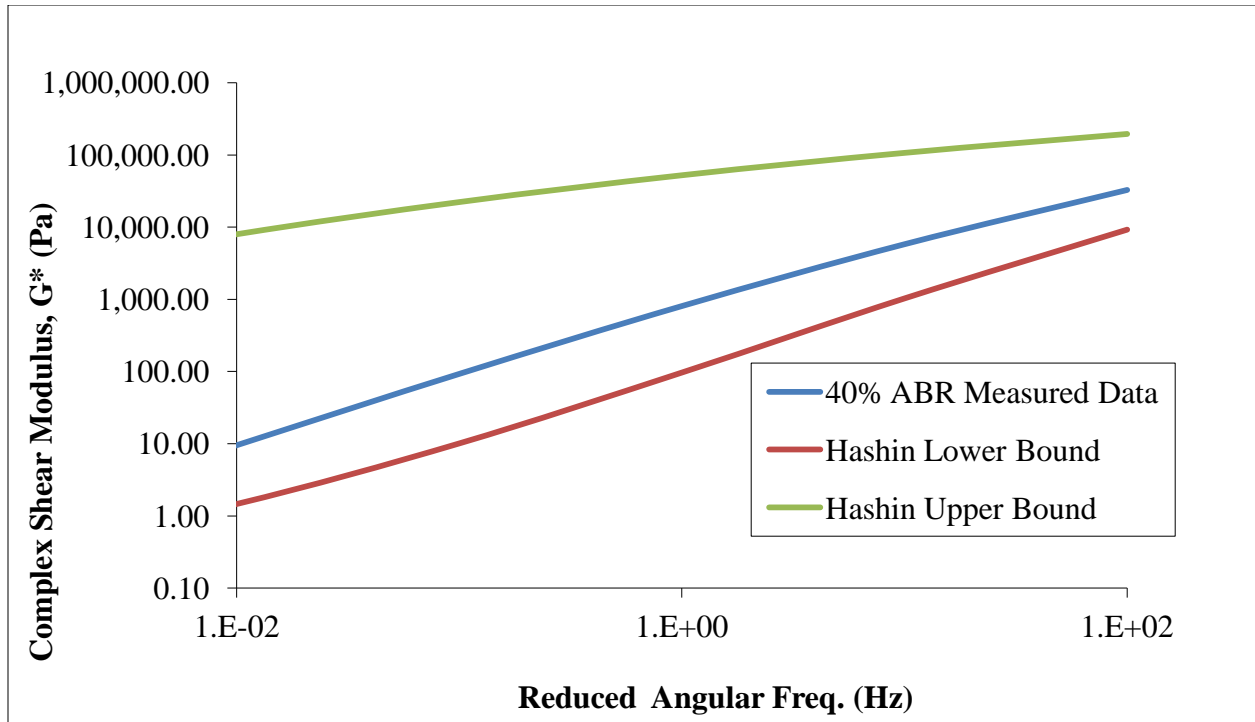


Figure 18. Complex Modulus Prediction of PG 46-34 with 40% RAS Binder Blending

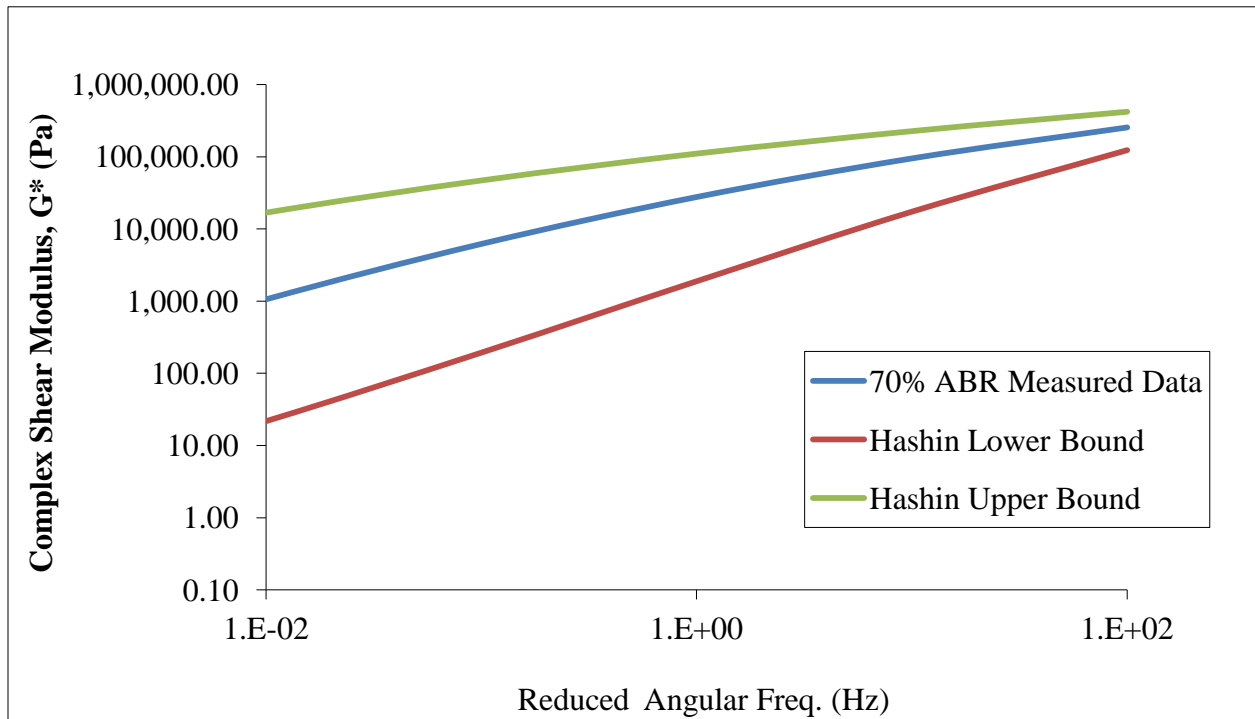


Figure 19. Complex Modulus Prediction of PG 46-34 with 70% RAS Binder Blending

4.2 Micromechanical Model Prediction of Creep Stiffness Master Curves

Hashin's and Shtrikman's Arbitrary Phase Model was used to derive a solution for creep stiffness at low temperatures. Equation 12 shows the common elastic parameter conversion from shear modulus to elastic modulus.

$$G = \frac{E}{2(1 + \nu)} \quad \text{Equation 12}$$

The BBR applies a load on a beam specimen and uses elementary bending beam theory to compute flexural creep stiffness. Therefore, Hashin and Shtrikman's Model must be modified to use the correct elastic parameter (elastic modulus). Equation 13 and Equation 14 show the full expanded lower bound and upper bound derivations respectively.

$$E_L = E_1 - \frac{2c_2(\nu_1 + 1)}{\frac{1}{\frac{E_1}{2\nu_1 + 2} - \frac{E_2}{2\nu_2 + 2}} - \frac{2c_1(\nu_1 + 1)\left(\frac{6E_1}{\nu_1 + 1} - \frac{2E_1}{(2\nu_1 - 1)}\right)}{5E_1\left(\frac{2E_1}{\nu_1 + 1} - \frac{E_1}{(2\nu_1 - 1)}\right)} \quad \text{Equation 13}$$

$$E_U = \frac{E_2}{2\nu_2 + 2} + \frac{2c_1(\nu_2 + 1)}{\frac{1}{\frac{E_1}{2\nu_1 + 2} - \frac{E_2}{2\nu_2 + 2}} - \frac{2c_2(\nu_2 + 1)\left(\frac{6E_2}{\nu_2 + 1} - \frac{2E_2}{(2\nu_2 - 1)}\right)}{5E_1\left(\frac{2E_2}{\nu_2 + 1} - \frac{E_2}{(2\nu_2 - 1)}\right)} \quad \text{Equation 14}$$

These derivations are in terms of the elastic modulus of phase one and phase two materials (E_1 and E_2), volume fractions of the two phases (c_1 and c_2) and the poisons ratios of the two phases (ν_1 and ν_2). With the assumption that the poisons ratios of the two materials are equal, the upper and lower bound simplify to the same equations shown previously for shear modulus and are reintroduced for elastic moduli bounds shown in Equation 15 and Equation 16 respectively.

$$E_L^* = E_1 + \frac{c_2}{\frac{1}{(E_2 - E_1)} + \frac{6(K_1 + 2E_1)c_1}{5E_1(3K_1 + 4E_1)}} \quad \text{Equation 15}$$

$$E_U^* = E_1 + \frac{c_1}{\frac{1}{(E_1 - E_2)} + \frac{6(K_2 + 2E_2)c_2}{5E_2(3K_2 + 4E_2)}} \quad \text{Equation 16}$$

The elastic moduli variables were replaced with the flexural creep stiffness master curve data obtained from the BBR test. Values for the creep stiffness phase one and phase two materials were obtained from the RAS and virgin binders based on the creep stiffness master curves shown previously. Upper and lower bound creep stiffness values were calculated for various reduced loading times.

4.2.1 Performance Graded 64-22 Base Binder

Flexural creep stiffness master curve data (at -12⁰C) was used for both the PG 64-22 and RAS binders to obtain upper and lower bound predictions. Figure 20, Figure 21, Figure 22, and Figure 23 show the prediction bounds and measured values for 10%, 20%, 40%, and 70% RAS binder blending percentages respectively. Consistently, the bounds underestimate the data. In addition, the two bounds show a very tight window for the predicted creep stiffness value, displaying a small difference between the upper and lower bounds. When Paul's Law of Mixtures Model was applied with the same data set, the bounds were slightly wider than Hashin and Shtrikman's Model, however still very tight. This unexpected bound prediction can be attributed to the small difference between the creep stiffness values obtained for the RAS and virgin binders. With the DSR, the difference in frequency values varied in magnitude on the order of 100,000, whereas the BBR creep stiffness values are not even one decade apart. However narrow, the bounds are still within the creep stiffness phase data supplied for both binders.

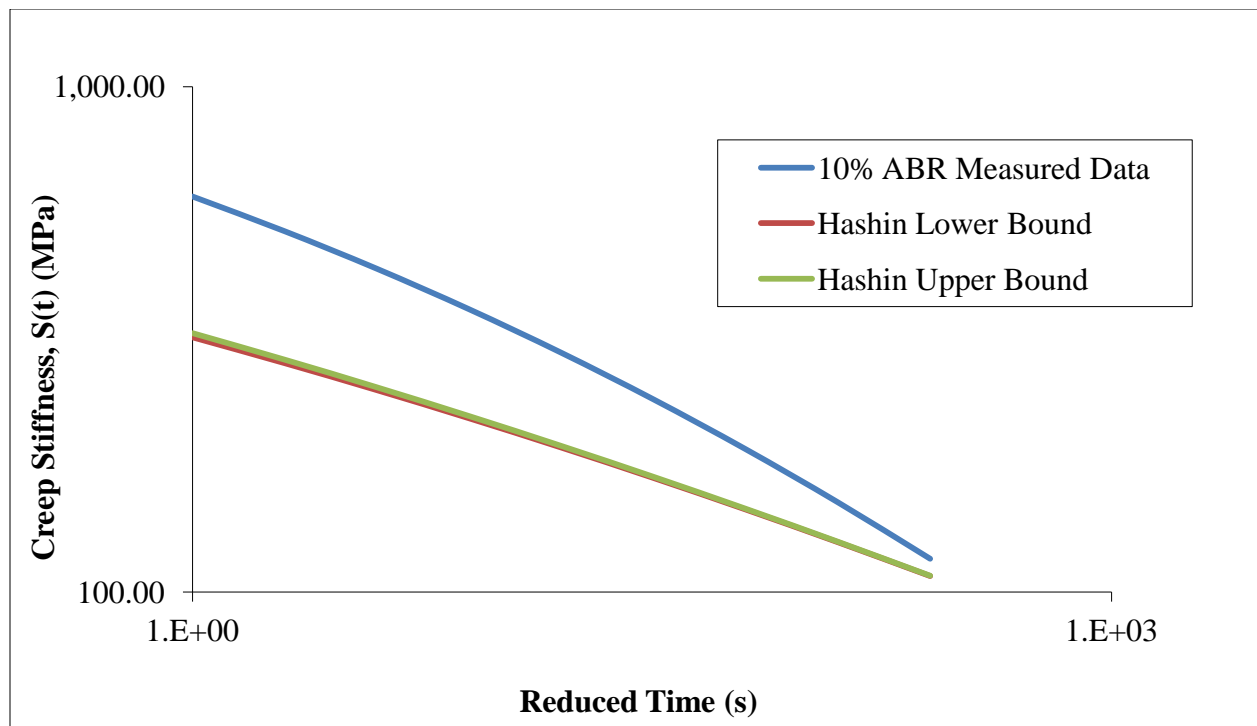


Figure 20. Creep Stiffness Prediction of PG 64-22 with 10% RAS Binder Blending

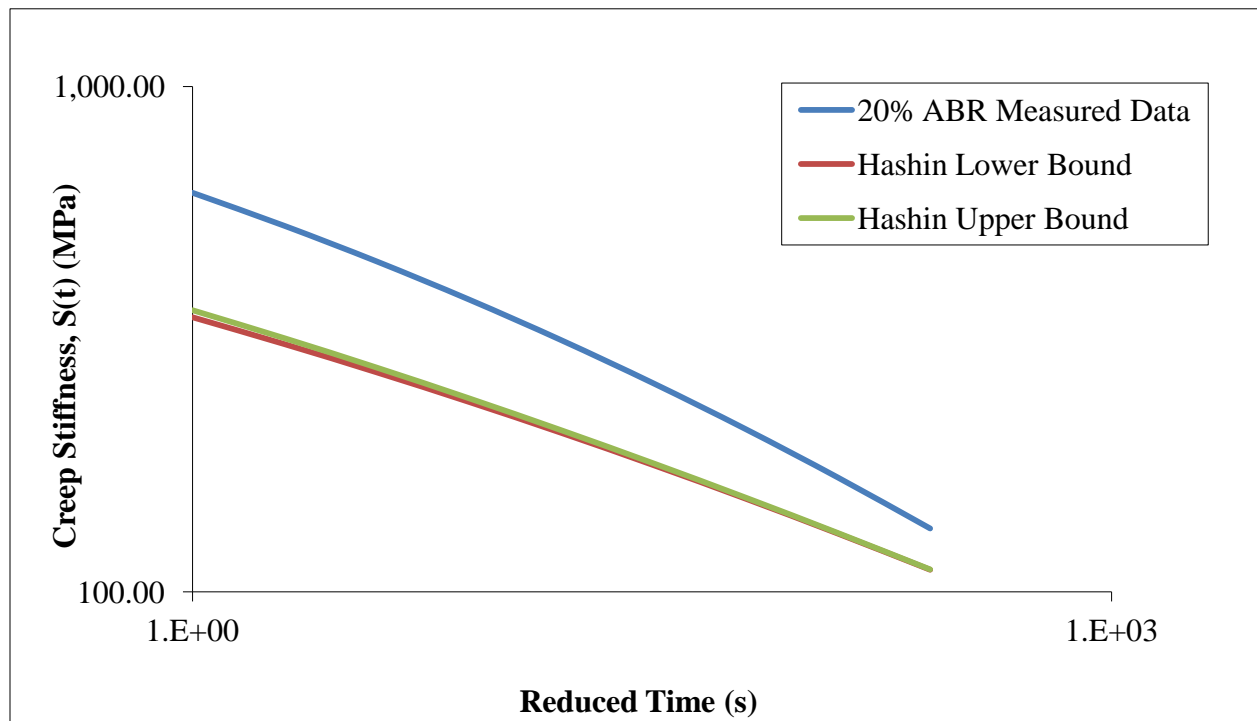


Figure 21. Creep Stiffness Prediction of PG 64-22 with 20% RAS Binder Blending

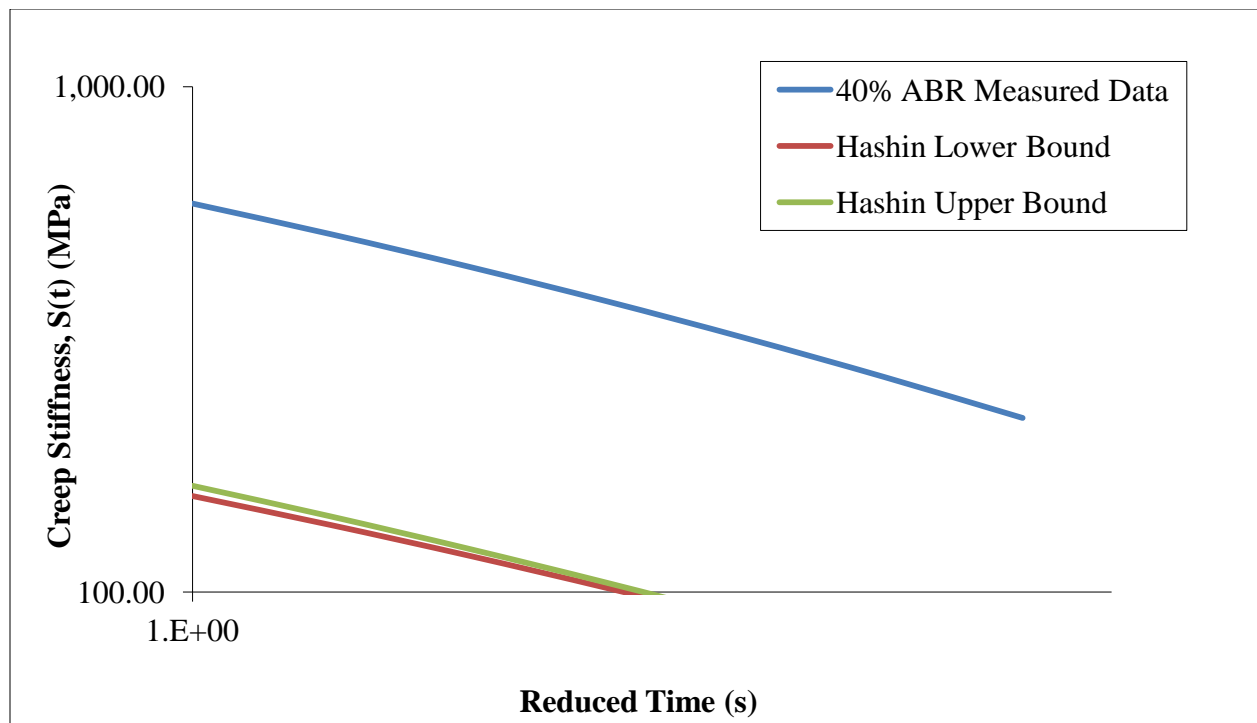


Figure 22. Creep Stiffness Prediction of PG 64-22 with 40% RAS Binder Blending

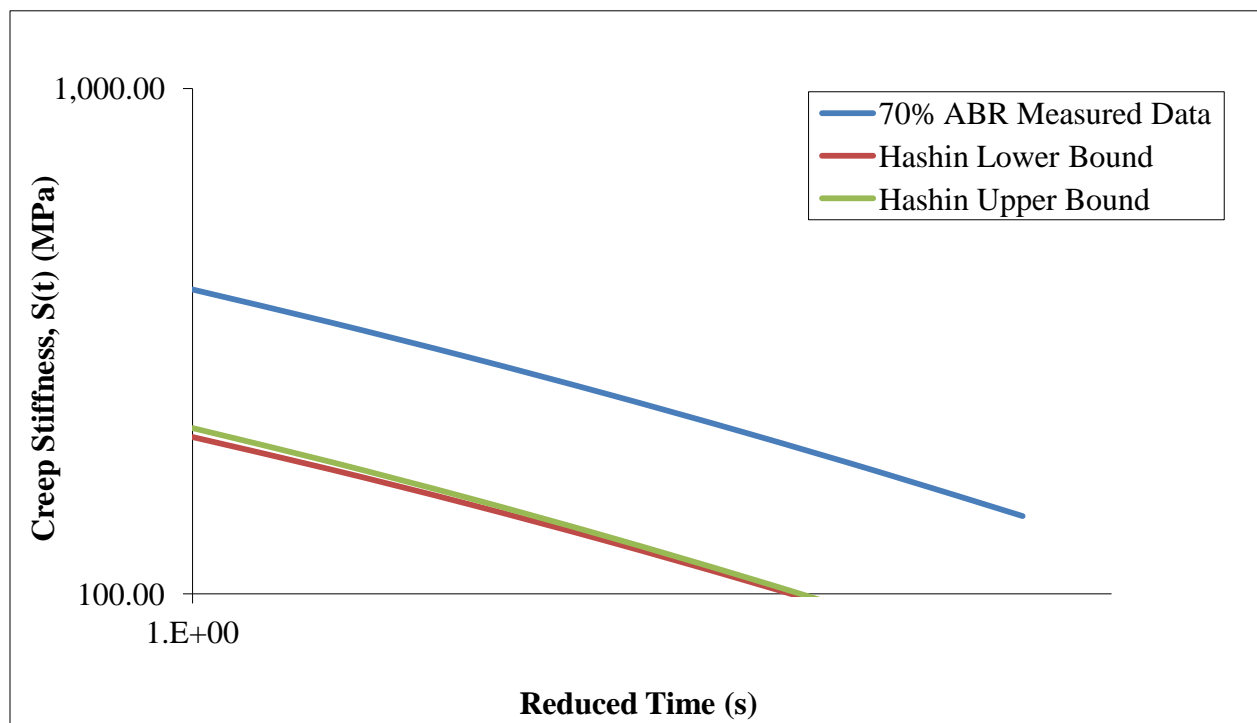


Figure 23. Creep Stiffness Prediction of PG 64-22 with 70% RAS Binder Blending

4.2.2 Performance Graded 46-34 Base Binder

The PG 46-34 binder creep stiffness master curve data (at -28°C) was used again with the RAS binder to obtain upper and lower bounds. The same observations reported for PG 64-22 were also seen for the 20%, 40% and 70% RAS binder blended with PG 46-34 binder shown in Figure 24, Figure 25 and Figure 26 respectively.

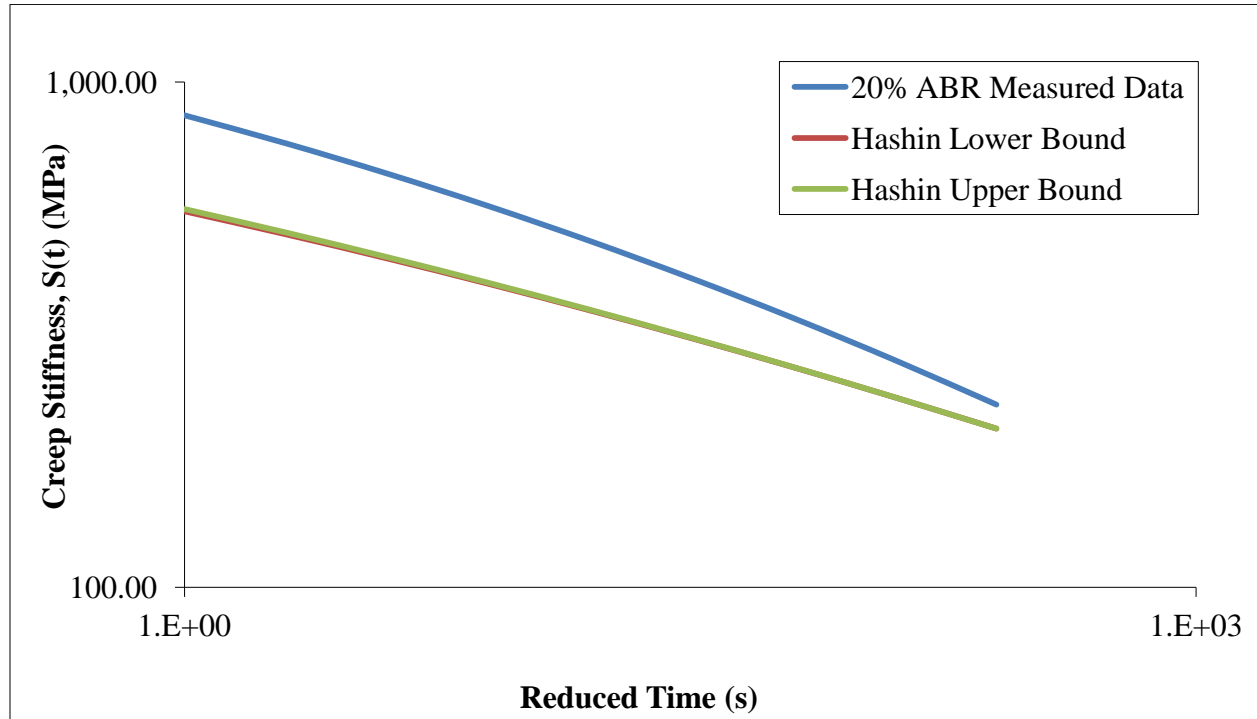


Figure 24. Creep Stiffness Prediction of PG 46-34 with 20% RAS Binder Blending

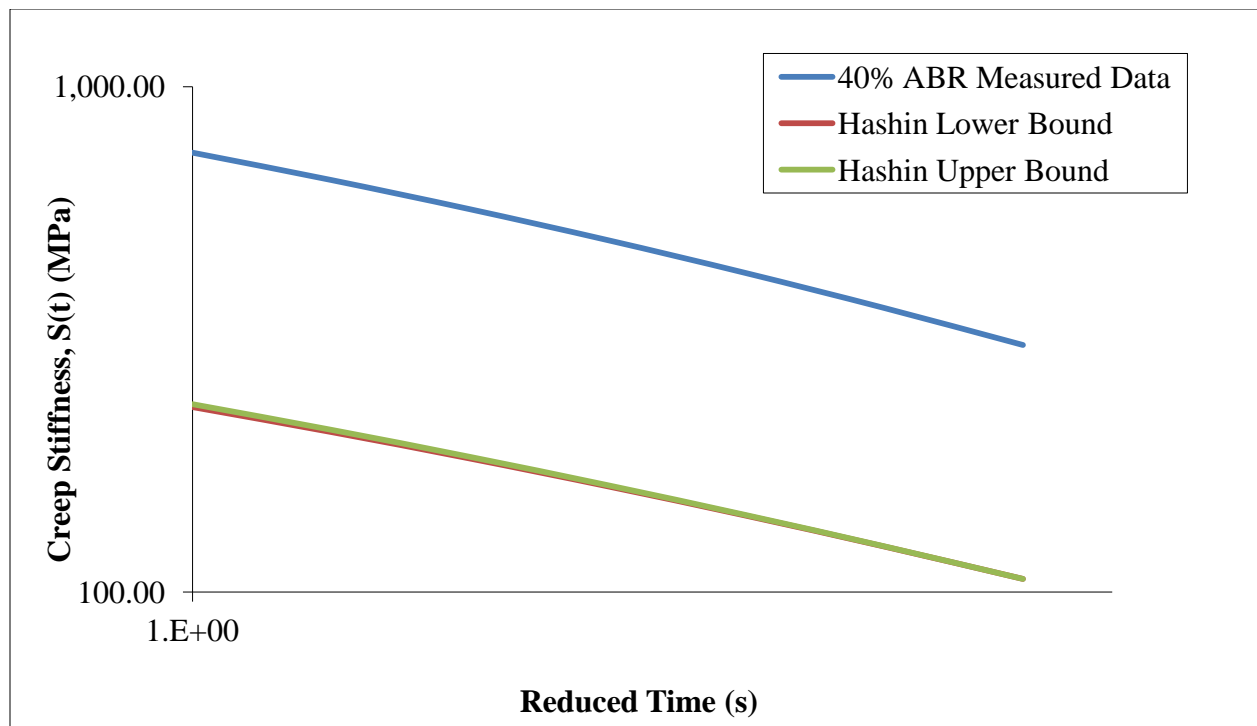


Figure 25. Creep Stiffness Prediction of PG 46-34 with 40% RAS Binder Blending

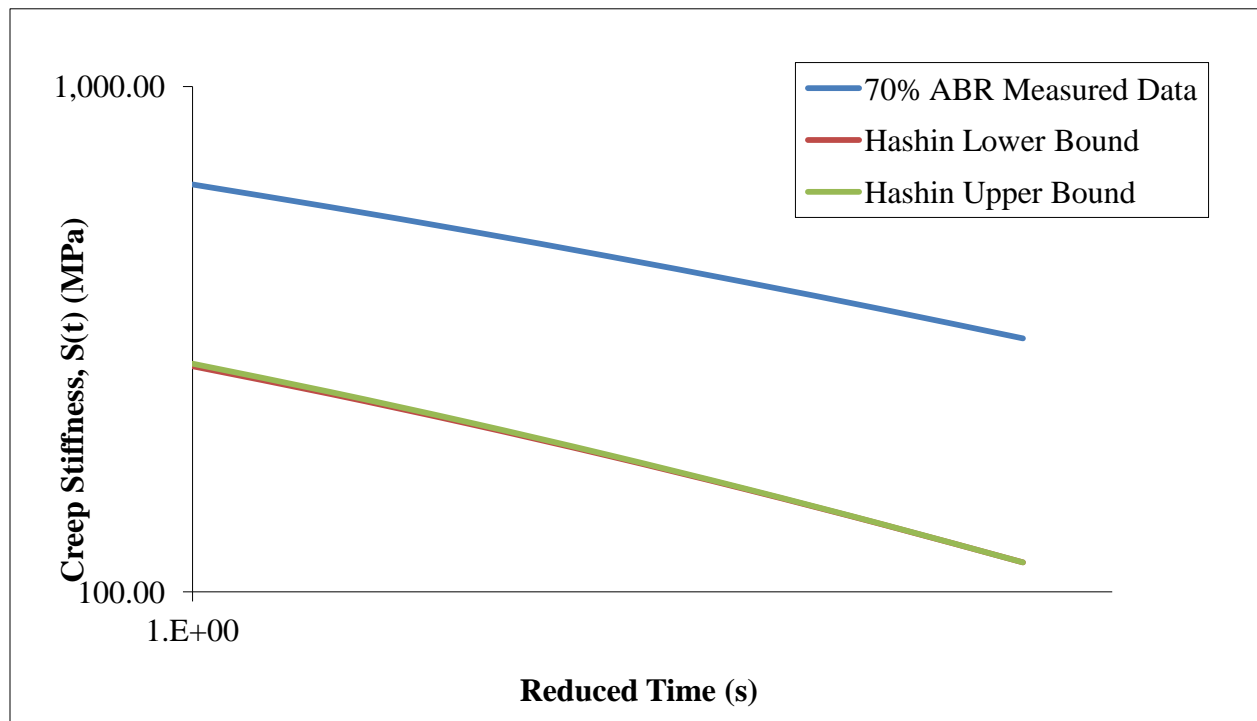


Figure 26. Creep Stiffness Prediction of PG 46-34 with 70% RAS Binder Blending

4.3 Use of Calibration Factors to Obtain Discrete Values

4.3.1 High Temperature Model Calibration

Calibration factors can be employed in order to predict a discrete value for complex shear modulus. The calibration scheme previously examined by Dave (12) was utilized for this study and is shown previously in Equation 9. The calibration factor S , is a value between 0 to 1; with 0 being the lower bound and 1 being the upper bound. The calibration factor varies across frequency, shown in Figure 27 for PG 64-22 with 10% RAS binder. Similar trends were noticed for other RAS binder blending percentages.

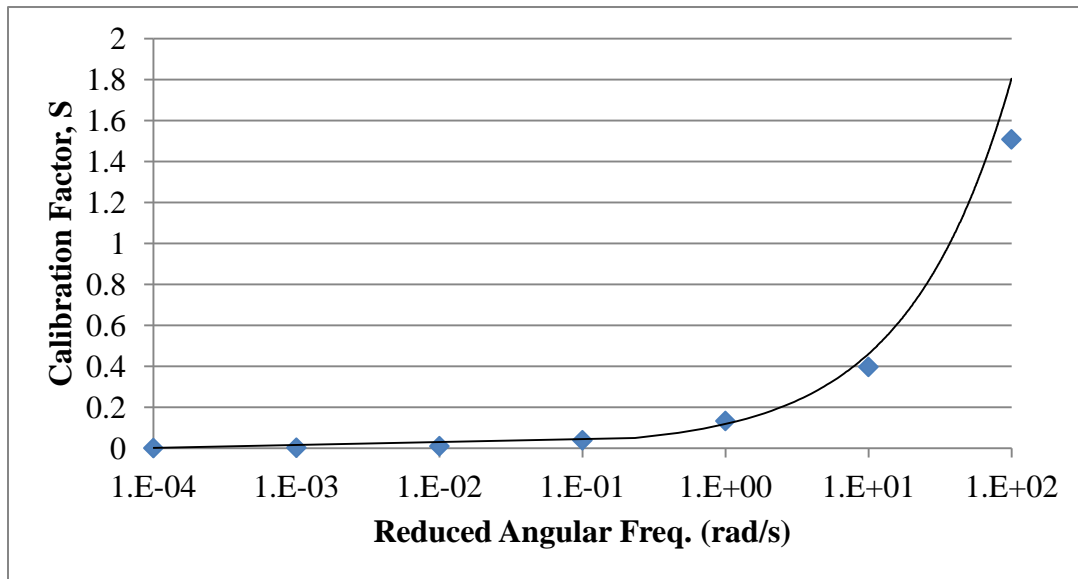


Figure 27. Calibration Factors for PG 64-22 blended with 10% RAS binder at 64°C

When observed on a log-log plot, the calibration factor increases exponentially which is an indication that as the angular frequency increases, the data becomes closer to the upper bound. Similar trends were observed for all binder blends. This calibration factor trend can be closely modeled using a power law, shown in Equation 17.

$$S = a\omega^b \quad \text{Equation 17}$$

Power law coefficients for all binder blends are shown in Table 7 and Table 8. The coefficients also vary across RAS binder blending percentages. This also indicates an indirect dependency of the calibration factor on the binder blending percentage.

Table 7. Coefficients for PG 64-22 Blended with RAS Binder

Power Law Coefficient	Percentage RAS Binder			
	10	20	40	70
a	0.005	0.024	0.106	0.202
b	0.650	0.530	0.434	0.279

Table 8. Coefficients for PG 46-34 Blended with RAS Binder

Power Law Coefficient	Percentage RAS Binder		
	20	40	70
a	0.003	0.012	0.202
b	0.637	0.552	0.279

Both power law coefficients generally show a linear dependency on RAS binder blending percentage. Variation of a-parameter and b-parameter with RAS binder blending percentage is shown in Figure 28 and Figure 29 respectively. No consistent trend can be observed when showing the direct dependency of the calibration factor on RAS binder blending percentage; however the calibration factor always increases with increasing angular frequency. An example of this trend is shown in Figure 30.

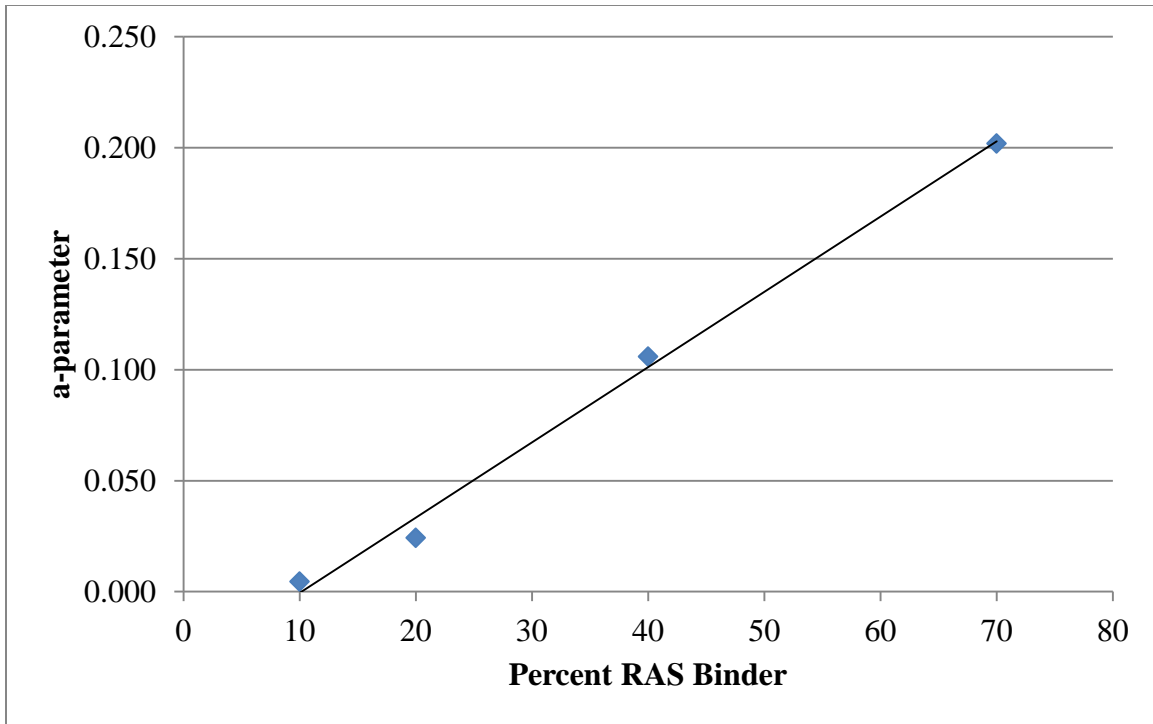


Figure 28. Variation of a-parameter for PG 64-22 blended with RAS Binder

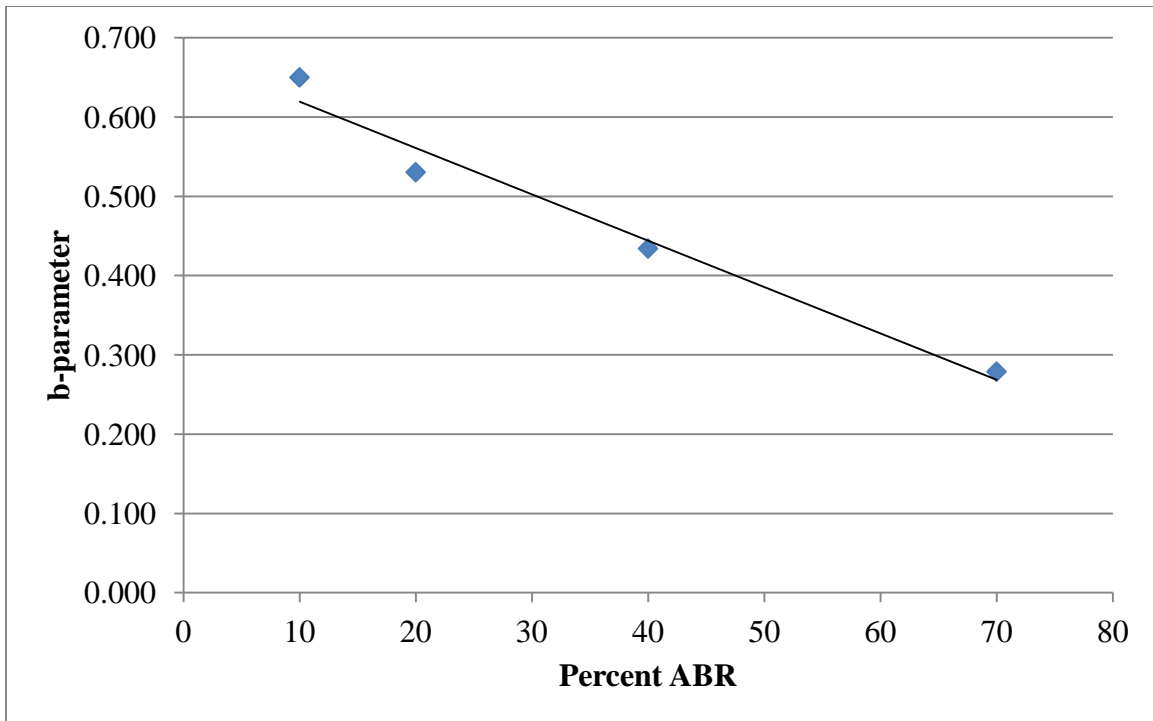


Figure 29. Variation of b-parameter for PG 64-22 blended with RAS Binder

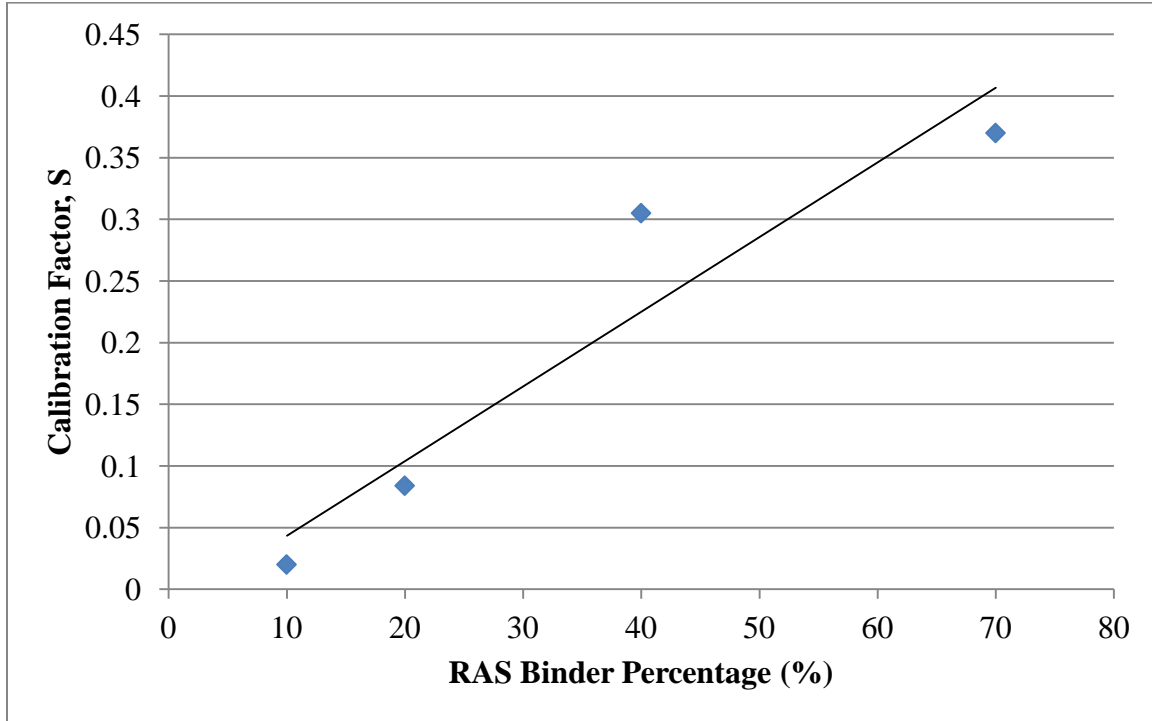


Figure 30. Calibration Factors for PG 64-22 blended with RAS Binder at 10 HZ, 64°C

The calibration factor is an indication of where the measured value is between the two bounds. Therefore, an increasing calibration factor indicates that the measured data is closer to the upper bound. The increasing calibration factor for both temperature and binder blending percentage indicates that the higher frequencies and RAS binder phases have an increasingly dominant effect on the complex shear modulus of the measured binder blend.

4.3.2 Low Temperature Model Calibration

An attempt was made to calibrate creep stiffness data. The same calibration factor equation used for the high temperature calibration (Equation 9) was used to calibrate the upper and lower bound creep stiffness curves at various reduced loading times. The calibration factor again varies across reduced time, shown in Figure 31. However, clearly this is not an appropriate use of a calibration factor as the measured creep stiffness data is significantly outside

the upper and lower bounds. Therefore, the calibrations factors are all greater than 1. At higher reduced loading times the calibration factor is as much as 2000 times the difference between the upper and lower bounds.

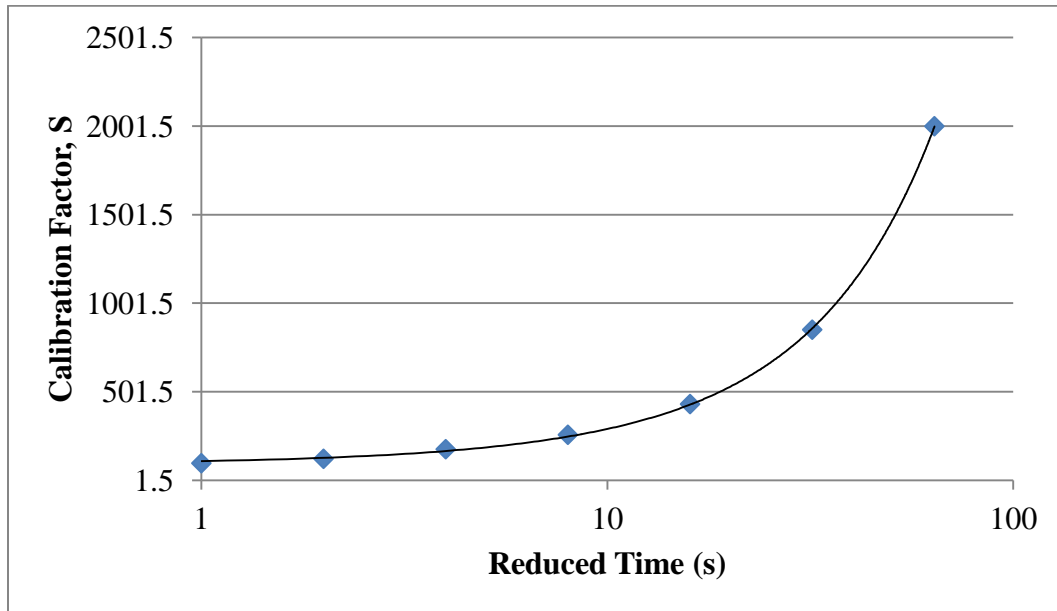


Figure 31. Calibration Factors for PG 46-34 blended with 70% RAS binder at -28°C

The calibration factor again follows a polynomial trend, indicating that the measured data consistently diverges away from the upper and lower bounds. This shows a more dominating virgin binder phase at lower temperatures.

Chapter 5: Summary

RAS binder contains very unique properties that make it very different from traditional virgin asphalt binder for which the Superpave performance grading system was developed. Therefore, a special forced oven air temperature controller used with a specially designed Dynamic Shear Rheometer must be utilized so material properties of RAS binder at high temperature can be characterized. In addition, RAS binder creates complications with low temperature binder testing using the BBR. A reduced load can be used to adequately obtain the necessary low temperature material properties. RAS and virgin binder were blended for two performance graded base binders: PG 64-22 and PG 46-34. High temperature complex shear modulus master curves and low temperature creep stiffness master curves give an indication of how RAS binder behaves and the influences it has on virgin binders. Performance grading at the high and low temperature ends also give an indication of acceptable average binder replacement that assumes total binder blending. Micromechanical models can be used to give a feasible prediction of RAS/virgin binder high temperature properties. Micromechanical models used at the low temperature end, however, do not feasibly predict the creep stiffness of RAS/virgin binder blends.

5.1 Conclusions

The following conclusions were drawn based on the conducted research:

- RAS binder has very unique characteristics
 - Complex shear modulus is significantly greater than available virgin asphalt binders
 - Flexural creep stiffness is softer at lower loading times and stiffer at greater loading times compared to available virgin asphalt binders

- Time-temperature dependency is reduced compared to most available virgin asphalt binders
- RAS/virgin binder blends show non-linear blending in terms of measured performance grade
- Hashin and Shtrikman's Arbitrary Phase Model can reasonably predict complex shear modulus values for blended RAS/virgin binders at high temperatures.
- Hashin and Shtrikman's Arbitrary Phase Model do not reasonably predict flexural creep stiffness values for blended RAS/virgin binders at low temperatures.

5.2 Recommendations

The following recommendations are made for continued work with RAS:

- A viscoelastic micromechanical model is needed for arbitrary phase composite materials such as RAS and virgin binder blends.
- RAP binder, warm mix additives and polymer modification needs to be investigated with RAS binder to determine the effect on Superpave material parameters.
- Although a performance grade may be determined for a given RAS/virgin binder blending percentage, the overall mixture performance should be evaluated as well. This is especially true for low temperature properties because RAS behaves as a stiff elastic material.

Chapter 6: References

1. **D'Angelo, J., et al.** *Warm-Mix Asphalt: European Practice*. 2008. FHWA Report No. FHWA-PL-08-007.
2. **McNulty, Raymond A.** *Asphalt Roofing Shingles - Composition, Performance, Function, and Standards*. s.l. : Interface, 2000.
3. **Zhou, Fujie, Button, Joe W. and Epps, Jon.** *Best Practice for Using RAS in HMA*. 2012. Report 0-6614-1.
4. *From Roofs to Roads ... Recycling Asphalt Roofing Shingles into Paving Materials*. Upper Marlboro, MD : National Association of Home Builders Research Center, 1998.
5. **Elseifi, Mostafa A., et al.** *New Approach to Recycling Asphalt Shingles in Hot-Mix Asphalt*. s.l. : Journal of Materials in Civil Engineering, 2012. Vol-24, pp. 1403-1411.
6. **Hasiba, Khaled I.** RAS Cost Analysis. *Southwind RAS LLC*. March 2013.
7. **Bonaquist, Ramon.** *Effect of Recovered Binders from Recycled Shingles and Increased RAP Percentages on Resultant Binder PG*. Madison : Wisconsin Department of Transportation, 2011. WHRP 11-13.
8. **Foxlow, Jennifer J., Daniel, Jo Sias and Swamy, Aravind Krishna.** *RAP or RAS? The Differences in Performance of HMA Containing Reclaimed Asphalt Pavement and Reclaimed Asphalt Shingles*. s.l. : Association of Asphalt Paving Technologists, 2011. Vol-80, pp. 347-376.
9. **Tran, Nam H., Taylor, Adam and Willis, Richard.** *Effect of Rejuvenator on Performance Properties of HMA Mixtures with High RAP and RAS Contents*. Auburn : National Center for Asphalt Technology, 2012. NCAT Report 12-05.

10. **Zhou, Fujie, et al.** *Recycled Asphalt Shingle Binder Characterization and Blending with Virgin Binders*. s.l. : Transportation Research Board, 2013. Paper 13-1810.
11. **Buttlar, William and Roque, Reynoldo.** *Evaluation of Empirical and Theoretical Models to Determine Asphalt Stiffness at Low Temperature*. s.l. : Association of Asphalt Paving Technologists, 1996. Vol-65, pp. 99-141.
12. **Dave, Eshan.** *Determination of Presence and Amount Recycled Asphalt Pavement in Asphalt Mixture*. Urbana : Graduate College of the University of Illinois at Urbana-Champaign, 2003. Thesis.
13. **Paul, B.** *Prediction of Elastic Constants of Multiphase Materials*. s.l. : Transactions of American Metallurgical Society, AIME, 1960. Vol-218, pp. 36-41.
14. **Hashin, Zvi and Shtrikman, S.** *A Variational Approach to the Theory of the Elastic Behaviour of Multiphase Materials*. s.l. : Journal of the Mechanics and Physics of Solids, 1962. Vol-11, pp. 127-140.
15. **Hashin, Z. and Shtrikman, S.** *On some Variation Principles in Anisotropic and Nonhomogeneous Material*. s.l. : Journal of Mechanics and Physics of Solids, 1962. Vol-10 pp. 355-342.
16. **Hashin, Z.** *The Elastic Moduli of Heterogeneous Materials*. s.l. : Journal of Applied Mechanics, 1962. Vol-29E, pp. 143-150.
17. **Christensen, R. M. and Lo, K. H.** *Solutions for Effective Shear Properties in Three Phase Sphere and Cylinder Models*. s.l. : Journal of Mechanics and Physics of Solids, 1979. Vol-27, pp. 315-330.
18. **Mori, T. and Tanaka, K.** *Average Stress in Matrix and Average Elastic Energy of Materials with Misfitting Inclusions*. s.l. : ACTA Metallurgica, 1973. Vol-21, pp. 571-574.

19. **Hirsch, T. J.** *Modulus of Elasticity of Concrete Affected by Elastic Moduli of Cement Paste Matrix and Aggregates*. s.l. : Journal of The American Concrete Institute, 1962. Vol-59-12, pp. 427-451.
20. **Buttlar, William G., et al.** *Understanding Asphalt Mastic Behaviour Through Micromechanics*. s.l. : Transportation Research Record, 1999. Vol-1681, pp. 157-169.
21. **Williams, M. L., Landel, R. F. and J., K. Ferry.** *The Temperature Dependence of Relaxation Mechanisms in Amorphous Polymers and Other Glass-Forming Liquids*. s.l. : The Journal of the American Chemical Society, 1955. Vol-77, pp. 3701-3707.
22. **Johnson, Eddie, et al.** *Incorporation of Recycled Asphalt Shingles in Hot-Mixed Asphalt Pavement Mixtures*. s.l. : Minnesota Department of Transportation, 2010. MN/RC 2010-08.
23. **Salari, Saman.** *Effects of Recycled Asphalt Shingle on the Rheological and Molecular Composition Properties of Asphalt Cement*. Baton Rouge : Louisiana State University, 2012. Thesis.